เส้นใยคอมพอสิตของพอลิ(3,4-เอทิลีนไดออกซีไทโอฟีน)และอนุพันธ์สำหรับการประยุกต์ทางเคมีไฟฟ้า

นายธนรัตน์ ภิสัชเพ็ญ

วิทยานิพนธ์นี้เป็นส่วนหนึ่งของการศึกษาตามหลักสูตรปริญญาวิทยาศาสตรดุษฎีบัณฑิต
สาขาวิชาเคมี ภาควิชาเคมี
คณะวิทยาศาสตร์ จุฬาลงกรณ์มหาวิทยาลัย
ปีการศึกษา 2560

COMPOSITE FIBER OF POLY(3,4-ETHYLENEDIOXYTHIOPHENE) AND DERIVATIVE FOR ELECTROCHEMICAL APPLICATIONS

Mr. Thanarath Pisuchpen

A Dissertation Submitted in Partial Fulfillment of the Requirements
for the Degree of Doctor of Philosophy Program in Chemistry
Department of Chemistry
Faculty of Science
Chulalongkorn University
Academic Year 2017

Thesis Title	COMPOSITE FIBER OF POLY(3,4-ETHYLENEDIOXYTHIOPHENE) AND DERIVATIVE FOR ELECTROCHEMICAL APPLICATIONS
By	Mr. Thanarath Pisuchpen
Field of Study	Chemistry
Thesis Advisor	Associate Professor Dr.Voravee Hoven
Thesis Co-Advisor	Assistant Professor Dr.Yongsak Sritana-anant Dr.Nadnudda Rodthongkum

Accepted by the Faculty of Science, Chulalongkorn University in Partial Fulfillment of the Requirements for the Doctoral Degree

.....Dean of the Faculty of Science
(Professor Dr.Polkit Sangvanich)

THESIS COMMITTEE

.....Chairman
(Associate Professor Dr.Vudhichai Parasuk)

.....Thesis Advisor
(Associate Professor Dr.Voravee Hoven)

.....Thesis Co-Advisor
(Assistant Professor Dr.Yongsak Sritana-anant)

.....Thesis Co-Advisor
(Dr.Nadnudda Rodthongkum)

.....Examiner
(Associate Professor Dr.Sumrit Wacharasindhu)

.....Examiner
(Professor Dr.Orawon Chailapakul)

.....External Examiner
(Dr.Varol Intasanta)

ธนรัตน์ ภิสัชเพ็ญ : เส้นใยคอมพอสิตของพอลิ(3,4-เอทิลีนไดออกซีไทโอฟีน)และอนุพันธ์สำหรับการประยุกต์ทางเคมีไฟฟ้า (COMPOSITE FIBER OF POLY(3,4-ETHYLENEDIOXYTHIOPHENE) AND DERIVATIVE FOR ELECTROCHEMICAL APPLICATIONS) อ.ที่ปรึกษาวิทยานิพนธ์หลัก: รศ. ดร.วรวีร์ โฮเว่น, อ.ที่ปรึกษาวิทยานิพนธ์ร่วม: ผศ. ดร.ยงศักดิ์ ศรีธนาอนันต์, ดร.นาฏนัดดา รอดทองคำ, 63 หน้า.

พอลิ(3,4-เอทิลีนไดออกซีไทโอฟีน) (PEDOT) เป็นพอลิเมอร์นำไฟฟ้าที่มีข้อดีหลายประการ เช่น มีค่าการนำไฟฟ้าสูง มีเสถียรภาพดีและมีความโปร่งแสง แต่ก็ยังมีปัญหาในด้านการละลายและไม่มีหมู่ฟังก์ชันที่เกิดปฏิกิริยากับสารอื่นๆได้โดยตรง โดยในงานวิจัยนี้ได้ทำการเตรียมเส้นใยคอมโพสิตที่มีองค์ประกอบของ PEDOT และพอลิเมอร์โดยปฏิกิริยาพอลิเมอไรเซชันในวัฏภาคของแข็งของ 2,5-ไดโบรโม-3,4-เอทิลีนไดออกซีไทโอฟีน (DBEDOT) และอนุพันธ์ที่มีหมู่คาร์บอกซิล (DBEDOT-C4-COOH) ร่วมกับเทคนิคอิเล็กโทรสปินนิง (electrospinning) เพื่อเพิ่มการกระจายของ PEDOT ในพอลิเมอร์เมทริกซ์ แผ่นเส้นใยคอมพอสิตที่ขึ้นรูปถูกนำไปดัดแปลงขั้วไฟฟ้าคาร์บอนเพื่อใช้ในการวิเคราะห์ทางเคมีไฟฟ้าเพื่อเป็นการประเมินศักยภาพในการนำไปประยุกต์ใช้ โดยแผ่นเส้นใยคอมพอสิต PEDOT และพอลิไวนิลแอลกอฮอล์ (PVA) สามารถเพิ่มการตอบสนองทางไฟฟ้าในเทคนิคไซคลิกโวลเทมเมตทรี (Cyclic Voltammetry) และการเพิ่มอนุภาคนาโนของเงินซึ่งเตรียมแบบเกิดขึ้นในระบบและหมู่คาร์บอกซิลจากอนุพันธ์ PEDOT-C4-COOH สามารถเพิ่มสัญญาณในการตรวจวัดไอออนสังกะสี แคดเมียม และตะกั่วพร้อมกันด้วยเทคนิคสแควร์-เวฟแอโนดิกสทริปปิงโวลแทมเมตรี (Square-wave anodic stripping voltammetry, SWASV) แต่ในการตรึงสารชีวโมเลกุลที่เป็นโพรบบนแผ่นเส้นใยยังไม่ประสบความสำเร็จต้องมีการปรับองค์ประกอบของเส้นใยต่อไป

ภาควิชา เคมี	ลายมือชื่อนิสิต .....
สาขาวิชา เคมี	ลายมือชื่อ อ.ที่ปรึกษาหลัก .....
ปีการศึกษา 2560	ลายมือชื่อ อ.ที่ปรึกษาร่วม .....
	ลายมือชื่อ อ.ที่ปรึกษาร่วม .....

5572817123 : MAJOR CHEMISTRY

KEYWORDS: POLY(3,4-ETHYLENEDIOXYTHIOPHENE) (PEDOT)/ POLY(VINYL ALCOHOL) (PVA)/ EMULSION ELECTROSPINNING/ CYCLIC VOLTAMMETRY (CV)/ SQUARE WAVE ANODIC STRIPPING VOLTAMMETRY (SWASV)/METAL DETECTION

THANARATH PISUCHPEN: COMPOSITE FIBER OF POLY(3,4-ETHYLENEDIOXYTHIOPHENE) AND DERIVATIVE FOR ELECTROCHEMICAL APPLICATIONS. ADVISOR: ASSOC. PROF. DR.VORAVEE HOVEN, CO-ADVISOR: ASSIST. PROF. DR.YONGSAK SRITANA-ANANT, DR.NADNUDDA RODTHONGKUM, 63 pp.

Poly(3,4-ethylenedioxythiophene) (PEDOT) is a conducting polymer that has many advantages including high conductivity, high transparency, and good stability. Despite its advantages, its insolubility and lack of active groups for further functionalization remain the major obstacles for its applications. In this work, polymer/PEDOT composite fibers were fabricated using solid state polymerization of 2,5-dibromo-3,4-ethylenedioxythiophene (DBEDOT) and its derivative containing carboxylic acid (DBEDOT-C4-COOH) in combination with electrospinning technique to ensure good dispersion of PEDOT in polymer matrix. The well-dispersed electrospun PEDOT/polymer composite the fiber mats were used to modify the screen-printed carbon electrode as testing models. The PEDOT/poly(vinyl alcohol) (PVA) composite fiber fabricated through emulsion electrospinning was found to increase the electrochemical response in cyclic voltammetry (CV), while an addition of silver nanoparticle generated *in situ* and carboxylic group via PEDOT-C4-COOH incorporation enhanced the electrochemical signal in simultaneous detection of Zn(II), Cd(II), and Pb(II) via square wave anodic stripping voltammetry (SWASV). An attempt to immobilize an enzyme onto the fiber-modified electrode was unsuccessful. Further adjustments on fiber composition are required.

Department:	Chemistry	Student's Signature	.....
Field of Study:	Chemistry	Advisor's Signature	.....
Academic Year:	2017	Co-Advisor's Signature	.....
		Co-Advisor's Signature	.....

ACKNOWLEDGEMENTS

First of all, I would like to express my heartfelt gratitude and appreciation to my advisor, Assoc. Prof. Dr. Voravee P. Hoven, for her support both in science and in life, and encouragement throughout the course of my study. I would also like to thank my co-advisors, Assist.Prof.Dr.Yongsak Sritana-anant and Dr.Nadnudda Rodthongkum, for their valuable suggestions.

I also would like to give my acknowledgement to Metallurgy and Materials Science Research Institute (MMRI) for the facility for the research. Many thanks go to all VH research group members for their assistance, suggestions concerning experimental techniques and their kind helps during my thesis work.

Finally, I would like to especially thank my family members: father, mother, younger sisters and relatives for their love, kindness and support throughout my entire study.

CONTENTS

Page

Page

Page

LIST OF FIGURES

Page

LIST OF TABLES

Page

CHAPTER I

INTRODUCTION

1.1 Statement of Problem and Literature Review

Conductive polymers are polymers with long range conjugated double bonds which allow electrons in the conjugated p-orbitals to become delocalized. When charge is introduced to the polymer through oxidation, or “doping”, the conjugated p-orbitals form an electronic band and the electrons within this band become mobile which allow the polymer to conduct electricity. Conductive polymers have been recently widely developed because of their outstanding properties as transparent and conductive materials, including polyacetylene, polyaniline, polypyrrole, polythiophene, poly(phenylenvinylene), and poly(paraphenylene). [1-2]

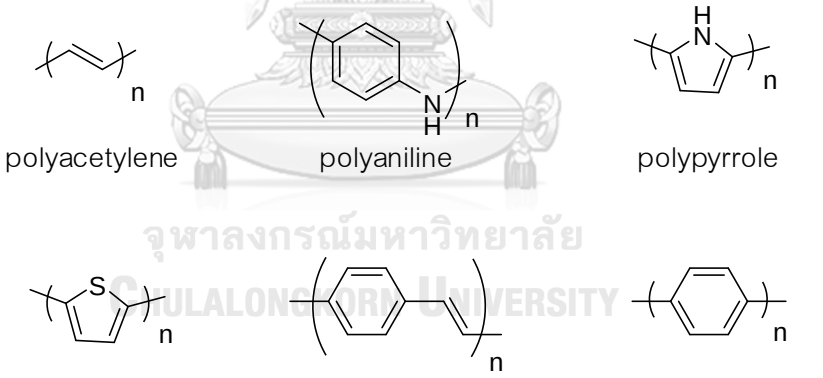

polyacetylene polyaniline polypyrrole

polythiophene poly(phenylenevinylene) poly(p-phenylene)

Figure 1.1 Structure of various conducting polymers

Poly(3,4-ethylenedioxythiophene) (PEDOT) is a polythiophene derivatives that was first manufactured by Bayer AG in 1980. [3] PEDOT has received much attention in recent years due to its high conductivity, high transparency, and good stability. [4] Processing of PEDOT, however, still have problem inherent in conductive polymer, namely being insoluble and infusible due to the stiffness of their all-conjugated

aromatic backbone structures and lacks of functional group that could increase solubility or allow for further modification. This problem was largely solved by performing polymerization of PEDOT onto the desired surfaces through oxidizing agent or electrochemical reaction with properties of PEDOT polymerized with oxidation being very dependent of counterion. [5] To overcome this problem, Groenendaal et al. first synthesized dispersion of PEDOT with polystyrene sulfonic acid (PEDOT:PSS) which is commercialized under the brand Baytron®P. Addition of PSS increase miscibility with solvent and increase conductivity, with PSS acting as dopant. [6] The tradeoff, however, is the acidity and hygroscopy of PSS, which can reduce the conductivity of PEDOT in humid environments and hamper its longevity.[7]

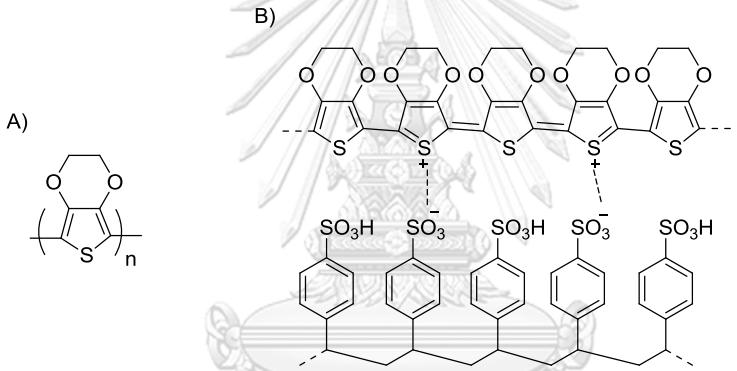

Figure 1.2 Structure of (A) PEDOT and (B) PEDOT:PSS

In 2003, Meng and coworkers [8-9] discovered that crystals of 2,5-dibromo-3,4-ethylenedioxythiophene (DBEDOT) could undergo solid state polymerization (SSP) after prolonged storage at room temperature or being heated below its melting point for several hours. This reaction could proceed without any initiators or catalysts and yield a nearly defect-free and highly ordered bromine-doped PEDOT with high conductivity.

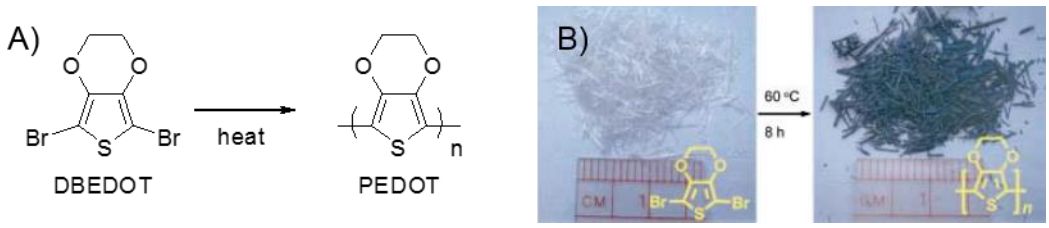

Figure 1.3 Solid state polymerization of DBEDOT (A) and color change of the solid monomer crystals (B). [8-9]

The example of applications of solid state polymerized PEDOT are as followed:

In 2013, Yin et al. [10] prepared PEDOT film by spin-coating the solution of DBEDOT onto the indium-tin oxide (ITO)-coated plastic electrode followed by heat treatment to convert DBEDOT into PEDOT. The electrode was evaluated for its potential as a counter electrode in solar cell. It was found that the energy conversion efficiency was 4.65% which was close to those of platinum electrode at 5.38%.

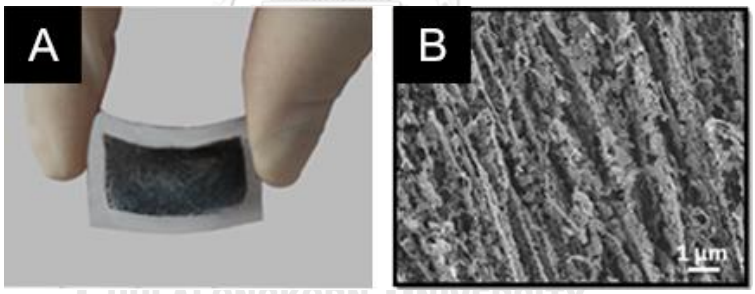

Figure 1.4 PEDOT-coated ITO plastic electrode (A) and the SEM micrograph of the surface of electrode. [10]

In 2016, McGraw et al. [11] prepared silicon nanoparticles-PEDOT (SiNPs-PEDOT) nanocomposites. By applying heat to a solution containing DBEDOT in acetonitrile with suspended silicon nanoparticles resulted in an *in situ* formed SiNPs-PEDOT nanocomposite with uniform dispersion of SiNPs in PEDOT matrix. The XRD, FTIR, and TGA analysis revealed that the addition of SiNPs was not an obstacle to the

polymerization of DBEDOT. The composite was used in the lithium-ion battery anode, in which the composite showed enhanced performance.

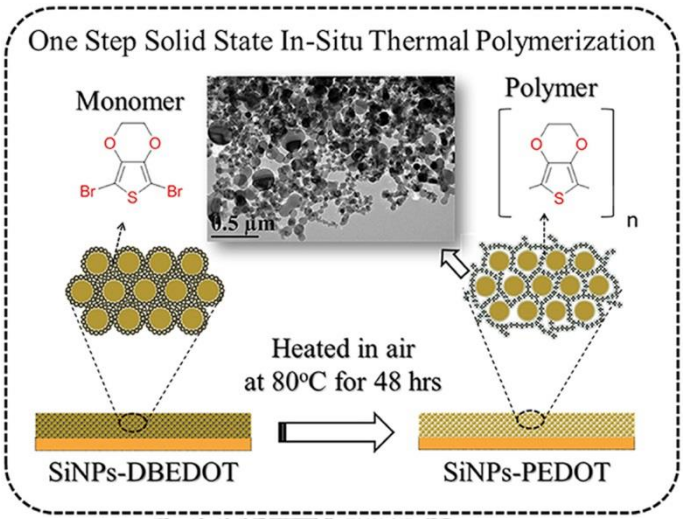

Figure 1.5 Preparation of SiNPs-PEDOT nanocoposite. [11]

In 2017, Yan et al. [12] prepared aligned carbon and graphite fibers with high crystallinity from PEDOT fibers synthesized through solid-state polymerization. Scanning electron microscopy showed that the graphite fibers have plate and layer morphologies in the through and edge directions, respectively, with good crystallinity. The conductivity of the graphite fibers was on the order of 100 S.cm−1 along the fiber axis.

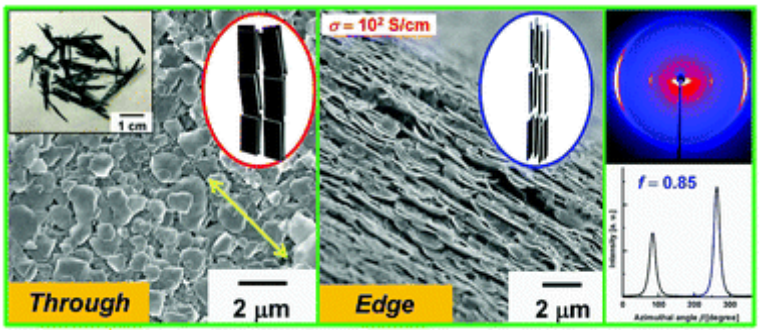

Figure 1.6 Graphite fibers prepared from solid state polymerized PEDOT. [12]

Previously, we applied this approach to fabricate the composite film of PEDOT and commercially available polymers, polystyrene (PS) and poly(methyl methacrylate) (PMMA), and sulfonated PS using electrospinning to prepare the thin fiber mat precursors, which transformed into conducting polymer film after heat treatment. PEDOT was found to be well-dispersed in polymer matrices. Furthermore, the conductivity of resulted films was higher than the film fabricated from commercially available PEDOT:PSS and comparable to those of pure solid-state polymerized PEDOT while still retained their conductivity even after 1- month storage. [13]

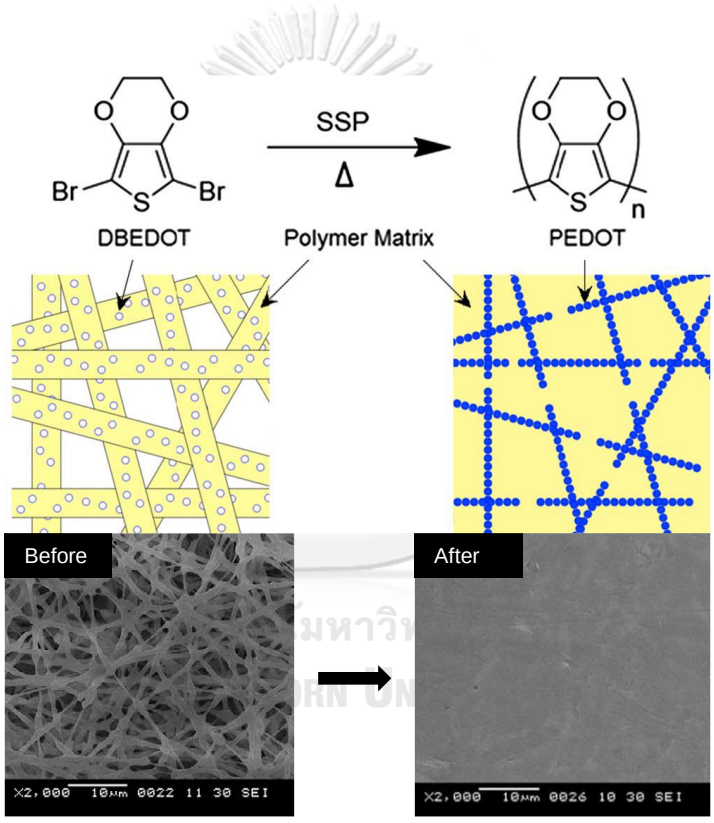

Figure 1.7 Schematic diagrams showing the solid-state polymerization of DBEDOT within the polymer matrix. [13]

Aside from dibromo derivative that could be used in solid state polymerization, other kinds of derivatives were synthesized in order to incorporate functional groups into PEDOT for various kind of applications, as in the following examples:

In 2014, Zhang et al. [14] synthesized EDOT derivative functionalized with carboxylic acid through the reaction between EDOT derivative containing hydroxyl group (hydroxymethyl EDOT) and succinic anhydride which was then polymerized on to the electrode through electropolymerization. The carboxylic group was used to enhance the detection of various amino compound including acetaminophen, quercetin, epinephrine, and tryptophan. The carboxylic group was also used to immobilize biomolecule probes, such as ascorbate oxidase (AO) for ascorbic acid detection.

In 2014, Hu *et al.* [15] synthesized EDOT derivative functionalized with benzoic acid which was then polymerized onto the electrode through electropolymerization. Not only this derivative could be used as electrochemical sensor, it could be used as optical sensor for various ions such as F^-, PO_4^{3-}, HCO_3^-, $S_2O_3^{2-}$, Cu^{2+}, and Fe^{3+}.

In 2015, Gulprasertrat *et al.* [16] synthesized DBEDOT derivative from hydroxymethyl EDOT and EDOT functionalized with toluenesulfonate group and chloroacetyl group. All derivatives could undergo solid state polymerization, with the resulted PEDOT derivative having high conductivity at 44.50 S/cm.

In 2016, Mawad *et al.* [17] synthesized PEDOT with functional pendant groups bearing double bonds which was employed in the fabrication of electroactive hydrogels with appropriate mechanical properties, electroactivity in physiological conditions, and suitability for proliferation and differentiation of C2C12 cells.

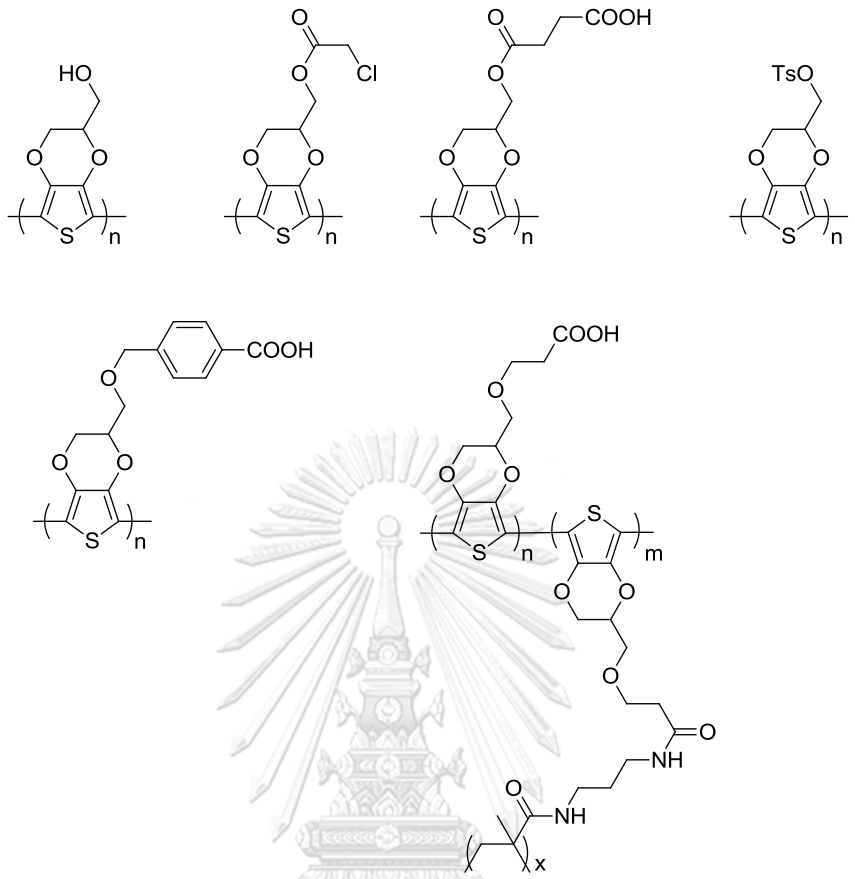

Figure 1.8 Structures of various PEDOT derivatives [14-17]

To further explore the possible applications for polymer/PEDOT composite films, we chose to fabricate polymer/PEDOT composite films for electrochemical analysis since it allowed us to monitor the properties of polymer/PEDOT composite without other outside factors. There were many previous works that involved PEDOT and electrospinning in fabrication of PEDOT fiber mats, but usually the fibers were used as template for PEDOT which was polymerized through oxidation, either by oxidizing agent or electrochemical reaction. The example of fabrication of PEDOT fibers through electrospinning are as followed:

In 2009, Bolin et al. [18] prepared polyethylene terephthalate (PET) electrospun fiber coated with PEDOT by first spin-coating the oxidizing agent, iron(III) tosylate, onto the fiber, followed by reaction between the oxidizing agent and EDOT vapor at 60°C.

The resulted PEDOT coated fiber had low resistivity at 1000Ω/square inch and could be used as a platform for growth and electrical stimulation of SH-SY5Y (Neuroblastoma) cell.

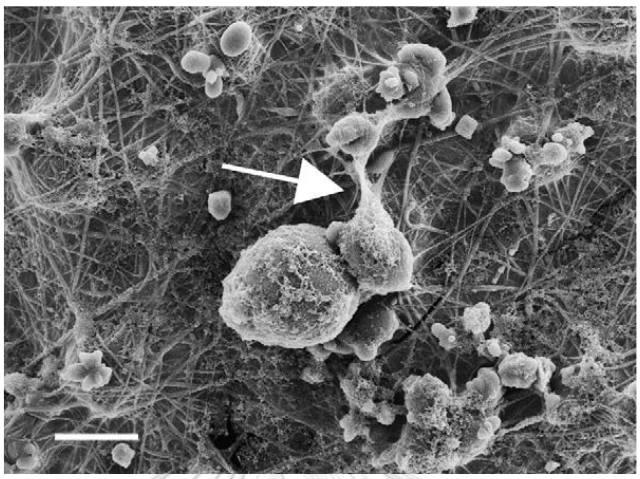

Figure 1.9 SEM micrograph of SH-SY5Y cells growing on PEDOT/PET fibers [18]

In 2013, Feng et al. [19] fabricated the microscale hollow PEDOT fiber through electrospinning of EDOT and poly(lactide-co-glycolide) (PLGA) composite polymer into iron(III) chloride solution in order to generate PEDOT on the surface of electrospun fiber, followed by dissolution of PLGA, resulted in hollow fiber with conductivity of 0.28 S/cm

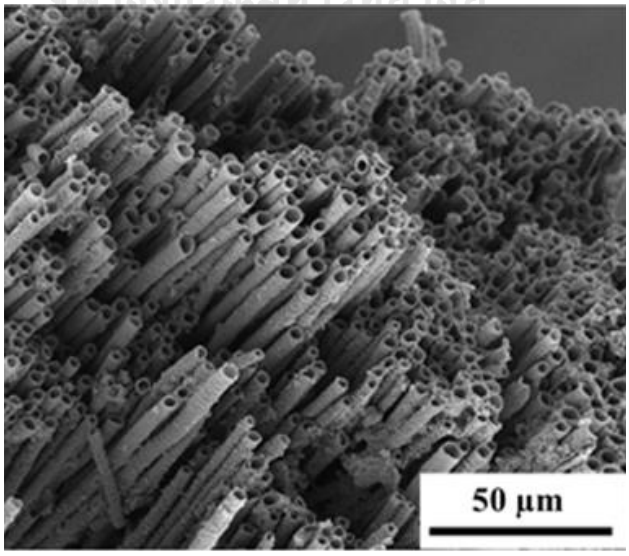

Figure 1.10 SEM micrograph of hollow PEDOT fibers [19]

In 2013, Yang et al. [20] prepared platinum electrode modified with PEDOT and entrapped glucose oxidase (GOx) by electropolymerization of EDOT onto flat surface and electrospun poly(L-lactide) (PLLA) fiber mat. It was found that by change the morphology from flat surface to fibers, the electrical impedance decreased from 111.2 ± 2 MΩ to 19.3 ± 5 MΩ. In the detection of glucose, the sensitivity increased from 1.2 ± 0.5 μA cm-2 mM-1 to 6.4 ± 0.7 μA cm-2 mM-1 and the LOD decreased from 0.56 mM to 0.26 mM.

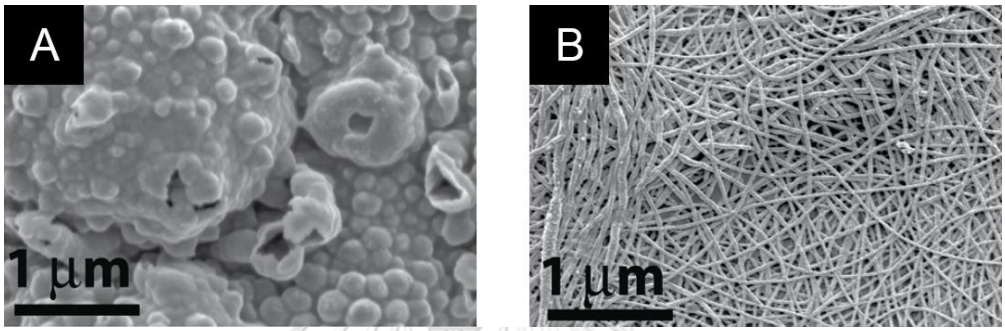

Figure 1.11 SEM micrograph of deposited PEDOT and entrapped GOx on the flat surface (A) and on PLLA fiber mat (B) [20]

The examples of applications of PEDOT in electrochemical analyses are as followed:

In 2012, Anastasova et al. [21] produced disposable solid-contact Pb^{2+}-selective-electrodes through electropolymerization of EDOT on screen-printed substrates for application as sensing devices for environmental monitoring of lead. The potentiometric measurements from the electrode correlate well with data determined using inductively coupled plasma mass spectrometry (ICP-MS) in the real sample.

In 2017, Li et al. [22] prepared composite on the screen-printed electrode that integrated molecular imprinting polymer for solid phase extraction (MISPE) technique for detection of tyramine. A linear concentration range of 5–100 nM with R^2=0.9939 was obtained with LOD and sensitivity at 2.31 nM and 3.11 μA nM^{-1} cm^{-2}, respectively.

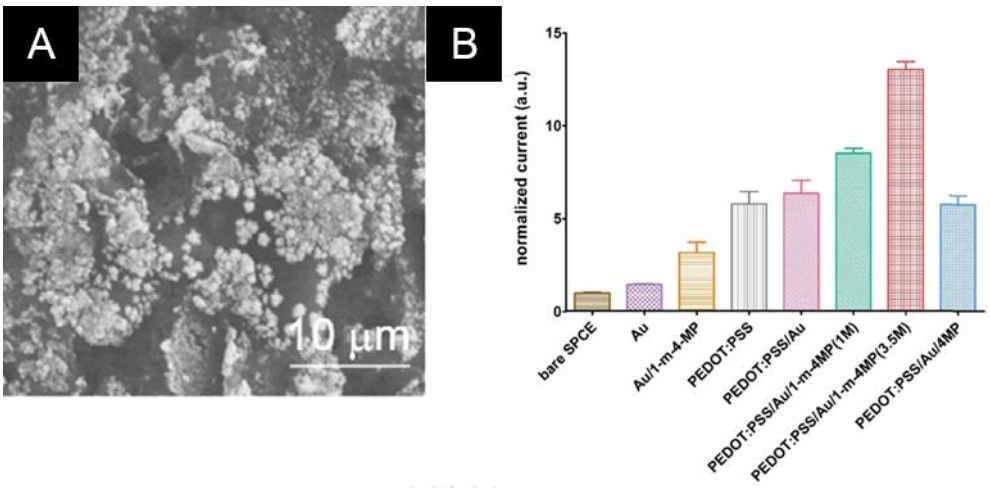

Figure 1.12 SEM micrograph of deposited PEDOT:PSS/AuNPs/1-m-4-MP composite (A) and electrochemical response from cyclic voltammetry of modified electrodes (B)

In 2018, Feito et al. [23] prepared PEDOT electrode by electropolymerization of PEDOT on platinum disc electrode and evaluate its potential in detection of short chain carboxylic acids, also known as volatile fatty acids (VFA) through pulse amperometric operation. Linear calibration curves with high correlation coefficients (>0.998) were obtained for sodium acetate, sodium propionate and sodium butyrate within the range of concentrations 0.1–10 mM. The PEDOT electrodes also remained stable and precise over at least one month without deterioration or loss sensitivity.

In 2018, Wong et al. [24] proposed a new sensor for the simultaneous determination of paracetamol (PAR) and levofloxacin (LEV), using a glassy carbon electrode (GCE) modified with AgNPs, carbon black (CB), and PEDOT:PSS through drop-casting the dispersion. The electrochemical behaviors of PAR and LEV were evaluated by cyclic voltammetry. Compared to the bare GCE, the modified sensor gave higher anodic peak currents, good linear concentration ranges and low detection limits of 1.2 × $10^{-8}$and 1.4 × 10^{-8} Mfor PAR and LEV, respectively. The AgNPs-CB-PEDOT:PSS/GCE sensor also displayed good stability, reproducibility, and repeatability, and no interference between of PAR and LEV.

To test the viability of SSP in fabrication of analytical devices, we aimed to use the ability of electrospinning to fabricate well-dispersed electrospun PEDOT/polymer composite fibers to modify on the screen-printed carbon electrode as testing models. Unlike in the previous work, in which the smooth films were formed, electrospun fibers have to retain its structure for the increased surface area. We also found that polymer that give the composite with highest conductivity was that from polar polymer, PMMA, instead of non-polar PS or polymer with charges like sulfonated PS. [13] Since the interface was designed to be used in aqueous media, polymer matrix should be hydrophilic but not water soluble in order to retain its fibrous morphology. As such, hydrophilic polymer, namely poly(vinyl alcohol) was chosen as the polymer matrix due to its electrospinning parameters being well documented [25-26] and its hydroxyl groups can be cross-linked. Additionally, hydroxyl group can also act as reducing agent for synthesis of metal nanoparticle such as silver nanoparticles (AgNPs), the components that help increasing electrochemical response. [27-28]

To fabricate the fibers with two immiscible phases of DBEDOT precursor and PVA, emulsion of DBEDOT solution and PVA solution was used to fabricate the composite fibers using the method similar to the one that was reported [29]. The electrospun fiber-modified electrode would then be tested for its potential as electrochemical electrode, including cyclic voltammetry (CV), square-wave anodic stripping voltammetry (SWASV). The carboxylic group-containing derivative would also be evaluated in its ability in immobilization of biomolecule to be used as detection probe.

1.2 Objective

To prepare and characterize PEDOT or derivative/polymer composite fiber mats by electrospinning and solid-state polymerization and evaluate electrodes modified by composite fiber mats in electrochemical applications

1.3 Scope of Investigation

The stepwise investigation was carried out as follows.

1. Literature survey for related research work
2. Synthesis of DBEDOT derivative containing carboxylic group
3. To prepare PEDOT or derivative/polymer composite fiber mats by electrospinning
4. Evaluate electrodes modified by composite fiber mats in electrochemical applications

Chapter II

EXPERIMENTAL

2.1 Materials

All reagents and materials are analytical grade (unless stated otherwise) and used without further purification.

1. 3,4-Ethylenedioxythiophene (EDOT) : Sigma-Aldrich
2. Hydroxymethyl EDOT : Sigma-Aldrich
3. N-bromosuccinimide (NBS) : Sigma-Aldrich
4. Pyridinium Tribromide : Sigma-Aldrich
5. 4-Dimethylaminopyridine (DMAP) : Sigma-Aldrich
6. Triethylamine : Sigma-Aldrich
7. Sodium Dodecylsulfate (SDS) : Sigma-Aldrich
8. Sodium Acetate (CH_3COONa) : Sigma-Aldrich
9. Potassium Ferricyanide ($K_3[Fe(CN)_6]$) : Sigma-Aldrich
10. Potassium Ferrocyanide ($K_4[Fe(CN)_6]$) : Sigma-Aldrich
11. 50% Glutaraldehyde solution : Sigma-Aldrich
12. Poly(vinyl alcohol) (PVA) (89-98 kDa, 99% hydrolyzed) : Sigma-Aldrich
13. Zinc(II) 1000 ppm Standard Solution : Sigma-Aldrich
14. Cadmium(II) 1000 ppm Standard Solution : Sigma-Aldrich
15. Lead (II) 1000 ppm Standard Solution : Sigma-Aldrich
16. Bismuth(III) 1000 ppm Standard Solution : Sigma-Aldrich
17. *N*-hydroxysuccinimide (NHS) : Sigma-Aldrich

18. Sodium Hydrogen Carbonate ($NaHCO_3$) : Merck

19. Sodium Sulfate (Na_2SO_4) : Merck

20. Sodium Chloride (NaCl) : Merck

21. Silver Nitrate ($AgNO_3$) : Merck

22. Acetic acid : Merck

23. Potassium chloride (KCl) : RFCL

24. 1-Ethyl-3-(3-dimethylaminopropyl)carbodiimide (EDC) : TCI

25. Dichloromethane (DCM) : RCI Labscan.

26. Toluene : RCI Labscan.

2.2 Equipments

2.2.1 Nuclear Magnetic Resonance Spectroscopy (NMR)

The ^1H NMR spectra were recorded in $CDCl_3$ using Varian, model Mercury-400 nuclear magnetic resonance operating at 400 MHz. Chemical Shifts (**δ**) are reported in part per million (ppm) relative to tetramethylsilane (TMS) or using the residual protonated solvent signal as reference.

2.2.2 Fourier Transform Infrared Spectroscopy (FT-IR)

The FT-IR spectra was recorded using Thermo Scientific Nicolet™ 6700. Solid samples were ground and mixed with anhydrous potassium bromide (KBr) in a mortar before compression to form KBr disk for characterization. Liquid samples were spread on NaCl window for characterization. The fiber mats on the electrode were characterized via attenuated total reflectance (ATR) mode.

2.2.3 Thermogravimetric Analysis (TGA).

The thermal degradation behavior of all polymer samples and the weight ratio of ash were investigated by thermogravimetric analysis (TGA) (Mettler Toledo, model TGA/SDTA 851^{e}, USA) over a temperature range of 30-600 ^{o}C at a heating rate of 10 ^{o}C/min under ambient conditions.

2.2.4 Scanning Electron Microscopy (SEM)

The morphological appearances of the as-spun fibers were investigated using a scanning electron microscope (SEM) model JSM-6480LV. Each sample was placed on the holder with an adhesive tape and coated with a thin layer of gold. The scanning electron images were obtained by using an acceleration voltage of 15kV. The average fiber diameter of the electrospun fibers was measured by Semafore software directly from SEM images.

2.2.5 Transmission Electron Microscopy (TEM)

The size and distribution of silver nanoparticles within the as-spun fibers were investigated using a transmission electron microscope (TEM) model Hitachi / S-4800. Each sample was prepared by electrospinning the fibers onto copper grid for 10 seconds. The transmission electron images were obtained by using an acceleration voltage of 100 kV. The average size of the silver nanoparticles was measured by Semafore software directly from TEM images.

2.2.6 X-ray Photoelectron Spectroscopy (XPS)

The XPS spectra were recorded using PHI 5000 VersaProbe III. X-ray was generated from aluminum anode (Al K**α**, 1486.6 eV) with beam diameter of 100 **μ**m and power of 100 W.

2.2.7 Electrospinning Equipment

The electrospinning process was performed under the electric field generated using high voltage power supply model Gamma High Voltage Research DES30PN/M692. The flow rate of polymer emulsion was controlled using syringe pump model ProSense NE 1000.

2.2.8 Electrochemical Analyses

All electrochemical analyses were performed on a μAUTOLAB type III potentiostat (Metrohm Siam Company Ltd.) controlled with the General Purpose Electrochemical System (GPES) software.

2.3 Synthesis of DBEDOT and derivative

2.3.1 Bromination of EDOT

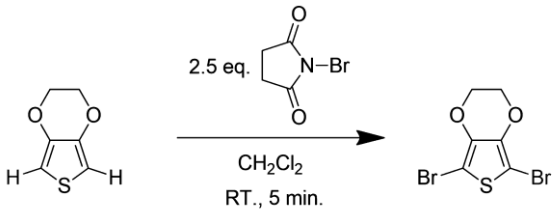

The bromination process was modified from a reported procedure. [16] NBS (0.890 g, 5 mmol) was dissolved in 10 mL DCM in 25 mL vial for 15 minutes. EDOT (0.214 mL, 2 mmol) was added via a micropipette while the solution was vigorously stirred. The reaction was carried out at room temperature for 5 minutes, after which the reaction was quenched by vigorous shaking of the mixture with saturated $NaHCO_3$ (10 mL) twice in a separation funnel. The aqueous phase was then extracted twice with DCM (10 mL) to recover the residual DBEDOT. The collected organic layer was washed twice with DI water, followed by partial evaporation to reduce the total volume to 10 mL. Residual bromine was then removed by column chromatography

using silica as stationary phase and eluted with mixed solvent of DCM and hexane (2:3 v/v). Finally, the product was obtained as white crystal after solvent evaporation via rotary evaporator. ^{1}H-NMR: **δ** (ppm) 4.3 ppm (s, CH_2CH_2), 80% yield)

2.3.2 Synthesis of Succinic anhydride-modified EDOT (EDOT-C4-COOH)

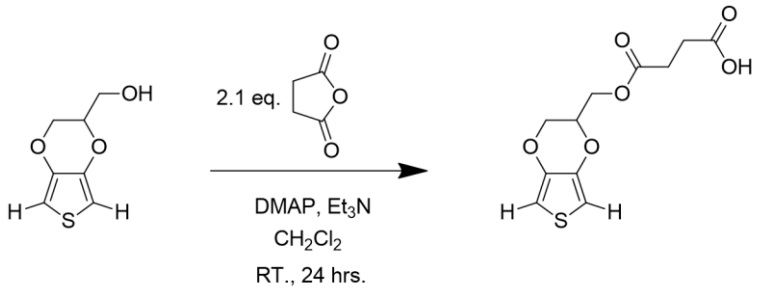

The synthesis procedure was modified from the previously reported method. [14] Hydroxymethyl EDOT (0.230 g 1.36 mmol) was dissolved in 5 mL of DCM in a 10 mL vial sealed with septum. Succinic anhydride (0.283 g, 2.83 mol), DMAP (12.3 mg, 0.12 mmol), and triethylamine (0.25 mL, 1.97 mmol) were dissolved in 12.3 mL of DCM in a 50 mL vial sealed with septum. After being purged with nitrogen gas for 15 minutes, hydroxymethyl EDOT solution was transferred to the second vial via purged syringe. The reaction was carried out under nitrogen atmosphere at room temperature for 24 hours. The reaction solution was then washed with 20 mL 1% HCl in brine 3 times and 20 mL of brine 5 times. The solution was dried over Na_2SO_4 followed by evaporation of solvent via rotary evaporator. ^{1}H-NMR: **δ** (ppm) 6.3 (s, 2Ar-H), 4.3 – 3.9 (m, CH_2CHCH_2), 2.6 (s, CH_2CH_2), 70% yield)

2.3.3 Bromination of EDOT-C4-COOH

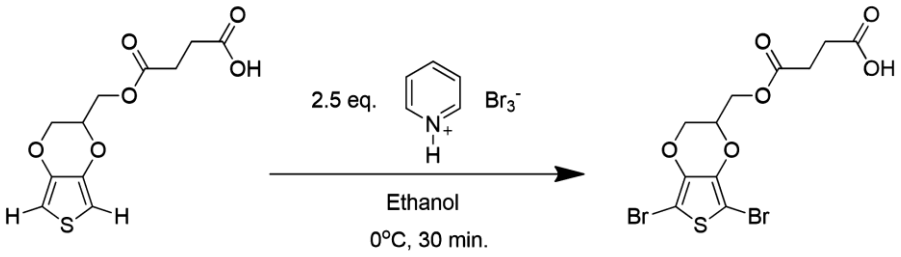

EDOT-C4-COOH (0.136 g, 0.50 mmol) was dissolved in 10 mL of ethanol in a 50 mL round bottom flask for 15 minutes at room temperature. Pyridinium tribromide (0.400 g, 1.25 mmol) was dissolved in 10 mL of ethanol in a 25 mL vial. EDOT-C4-COOH solution was then cooled to 0oC in ice bath, followed by addition of pyridinium tribromide solution dropwise. The reaction was carried out at 0oC for 30 minutes, after which the reaction was quenched by addition of 50 mL of DCM and vigorous shaking of the mixture with 1% HCl in brine (10 mL) twice in a separation funnel. The aqueous phase was then extracted twice with DCM (10 mL) to recover the residual product. The collected organic layer was washed 5 time with 20 mL of brine. Finally, the product was obtained as brown solid after solvent evaporation via rotary evaporator. 1H-NMR: **δ** (ppm) 4.4 – 4.0 (m, CH2CHCH2), 2.6 (s, CH2CH2), 60% yield)

2.4 Preparation of PVA Solution and Simultaneous Formation of Silver Nanoparticles (AgNPs)

PVA solution was prepared by dissolving 1.2 g of PVA in DI water at the concentration of 12% w/w. SDS (0.012 g, 1% by weight of PVA) was added and the mixture was stirred and heated at 80°C for 24 hours to ensure the homogeneity of the solution. AgNPs in PVA solution was prepared by adding $AgNO_3$ (0.012 g, 1% by weight of PVA) to the PVA and SDS mixture above before heating, yielding transparent yellow-brown solution.

2.5 Fabrication of Screen-printed Carbon Electrode

The screen-printed carbon electrodes were prepared using an in-house screen-printing technique. The screen-printed carbon electrode patterns were designed in Adobe Illustrator (**Figure 2.1**). First, the silver/silver chloride (Ag/AgCl) ink was screened onto a poly(vinyl chloride) (PVC) substrate to form the conductive layer to connect with electrochemical detection part. Then, the carbon ink was screened onto the same PVC substrate twice as the second layer to obtain the screen-printed carbon electrodes. These electrodes were dried in an oven at 55 °C for 1 hour after each screen-printing and stored in a desiccator at room temperature until used.

Figure 2.1 Screen printing block for Ag/AgCl Ink (left) and Carbon Ink (right)

2.6 Electrospinning of Composite Fiber and Treatments

DBEDOT solution was prepared by dissolving DBEDOT in toluene at the concentration of 40% w/w. PVA or PVA-AgNP solution was then vigorously mixed with DBEDOT solution in the ratio of 2:1 v/v to form emulsion. In the case of DBEDOT-C4-COOH, the amount of DBEDOT above was replaced with DBEDOT and DBEDOT-C4-COOH at 1:1 ratio in equivalence. Each of the as-prepared emulsions was then placed in a 3-mL syringe having a 1.5-cm long blunt 20-gauge stainless steel hypodermic needle as a nozzle which was connected with the positive electrode. The syringe was placed on the syringe pump with a flow rate of 1.5 mL/hour. A grounded rotary cylinder covered by carbon based electrode and aluminum foil was used as the counter

electrode and was placed 15 cm away from the tip of the needle and rotate at the speed of 300 rpm. Composite fiber mats were fabricated by electrospinning an emulsion at ambient temperature using a driving voltage of 15 kV. An apparatus set-up for electrospinning is shown in **Figure 2.2**. The spinning was performed for 5-50 minutes, and then the electrodes covered with electrospun fibers were exposed to glutaraldehyde vapor from 50% glutaraldehyde solution in closed container for cross-linking of PVA for 24 hours, followed by heat treatment in an oven at 70°C for 48 hours to induce solid state polymerization of DBEDOT into PEDOT.

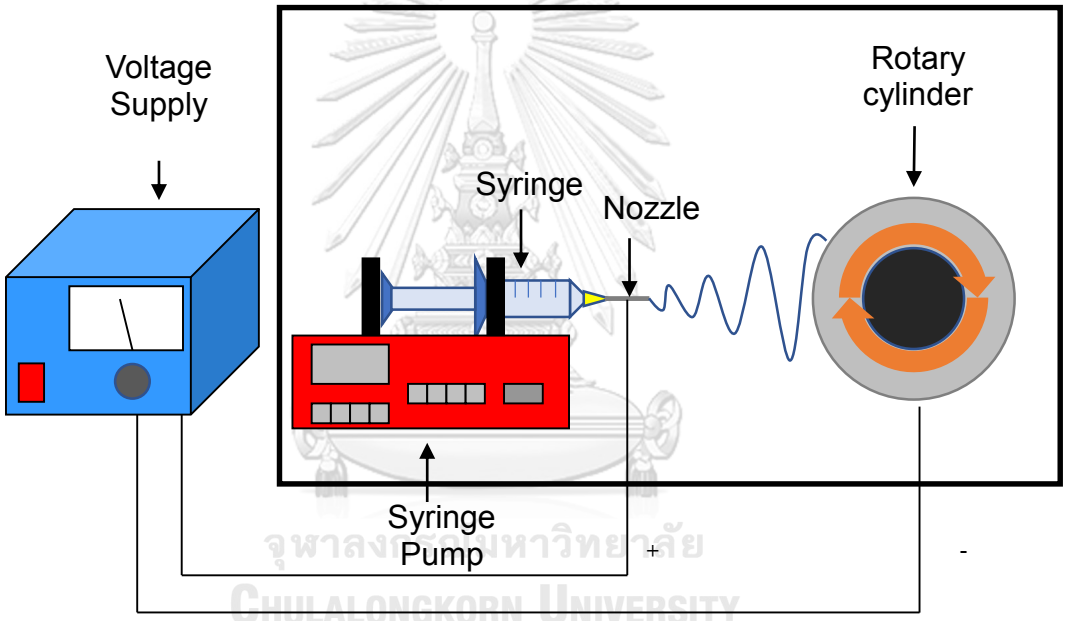

Figure 2.2 Apparatus set-up for electrospinning

2.7 Immobilization of Glucose Oxidase (GOx)

GOx was immobilized onto the electrospun PEDOT-C4-COOH/PVA composite fiber on the electrode through coupling with carboxyl group using EDC/NHS coupling agent. The electrodes modified by PEDOT-C4-COOH/PVA composite fiber were submerged in a 0.1 mM PBS containing 0.2 mM EDC and 0.05 mM NHS. The reaction was stirred for 30 minutes, followed by addition GOx, with final concentration in the bulk solution at 1 mg/mL. The reaction was kept at 25°C for 24 hours, after which the

electrodes were washed by DI water twice and dried in the air under ambient temperature.

2.8 Electrochemical Analyses

The configuration of an in-house electrochemical cell is shown in **Figure 2.3**. The composite fiber-modified screen-printed carbon electrodes were used as the working electrode (WE), and the area of the electrode exposed to the solution was limited to the circle with a diameter of 0.4 cm. A Pt wire and Ag/AgCl were used as the counter electrode (CE) and reference electrode (RE), respectively. For all electrochemical measurements, the analyte solution volume was limited to 3 mL in a well (diameter 2.5 cm and height 2.0 cm).

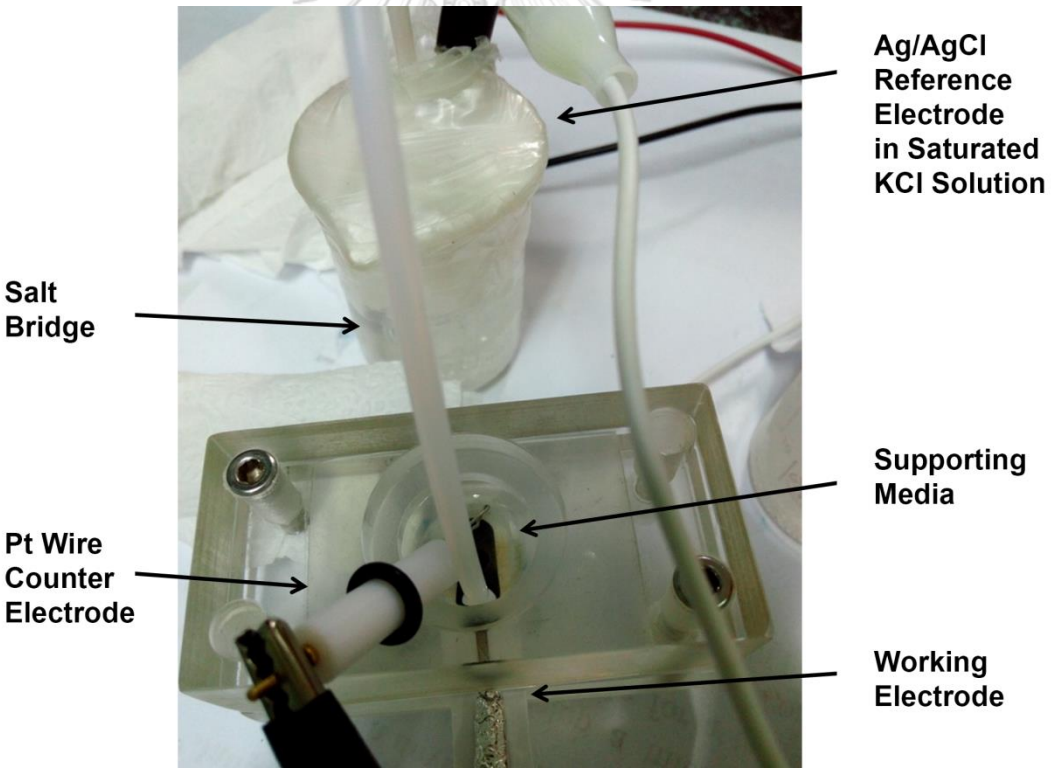

Figure 2.3 Electrochemical cell set-up

2.8.1 Cyclic Voltammetry (CV)

The CV measurements were performed over a potential range from -0.5 to +1.0 V at a scan rate of 100 mV/s. 3 mL of 1 mM $K_3[Fe(CN)_6]/K_4[Fe(CN)_6]$ (1:1 molar ratio) in 0.1 M KCl solution was used as the electrolyte.

2.8.2 Square Wave Anodic Stripping Voltammetry (SWASV)

In SWASV, the deposition was performed at -1.6 V and the scan was performed from -1.6 to 0.25 V with step potential of 0.01 V, amplitude of 0.04 V, and frequency of 35 Hz. 3 mL of 0.1 M acetate buffer solution (pH 4.6) was used as a supporting electrolyte. Varied amount of 10 ppm Zn(II), Cd(II), and Pb(II) standard solution was spiked into the supporting solution to achieve the concentration from 10 to 80 ppb. Varied amount of 10 ppm Bi(III) standard solution was then spiked into the supporting solution to achieve the concentration from 100 to 500 ppb.

2.8.3 Amperometry

The amperometry measurements were performed by varying the potential over the range from -1.0 to +1.0 V. Each measurement was taken with constant potential over 120 seconds. 3 mL of 0.1 mM phosphate buffer solution (PBS) was used as an electrolyte.

Chapter III

RESULTS AND DISCUSSION

3.1 Syntheses of DBEDOT and Derivatives

3.1.1 Synthesis of DBEDOT

DBEDOT was synthesized by bromination of EDOT. The success was confirmed through ^{1}H-NMR analysis with disappearance of a peak at 6.3 ppm, which represents EDOT's thiophene protons (peak a in **Figure 3.1**). The shift of ethylene protons from 4.2 ppm in EDOT (peak b in **Figure 3.1**) to 4.3 ppm in DBEDOT (peak c in **Figure 3.1**) could be explained with the inclusion of electron withdrawing bromo groups. The product was obtained as white crystal after solvent evaporation in 80% yield.

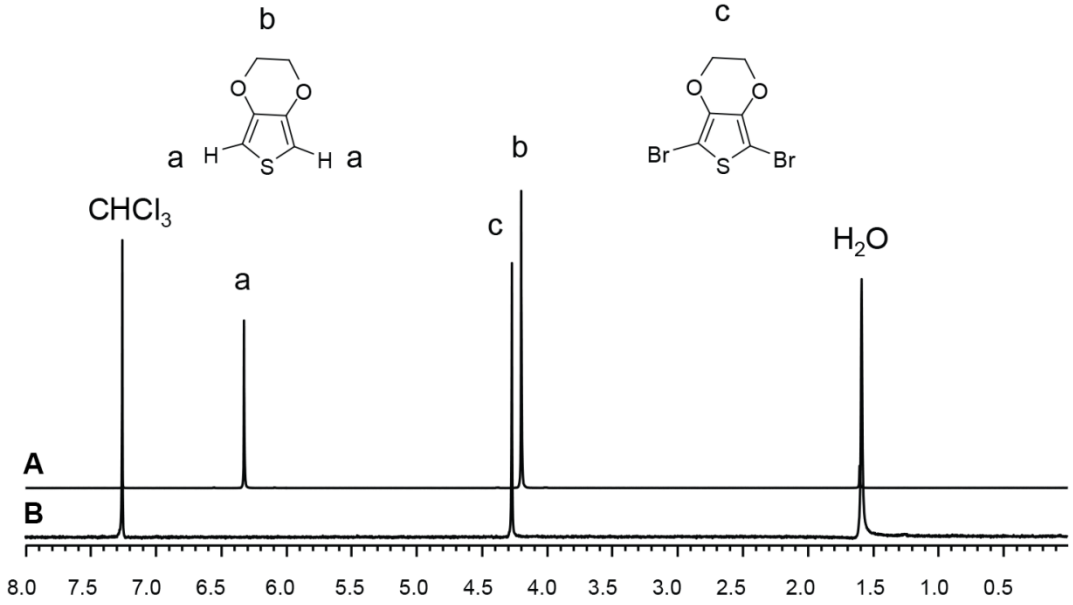

Figure 3.1 ^{1}H NMR spectra of (A) EDOT and (B) DBEDOT.

3.1.2 Synthesis of EDOT-C4-COOH

Characterization of EDOT-C4-COOH synthesized from hydroxymethyl EDOT and succinic anhydride was performed by ^{1}H-NMR and FT-IR analysis. In ^{1}H NMR spectra shown in **Figure 3.2**, complete disappearance of a peak at 1.9 ppm, which is assigned to hydroxymethyl EDOT's hydroxyl protons (peak e) and appearance of a new peak at 2.6 ppm (peak e') which could be attributed to methylene protons of succinate ester, confirmed that hydroxy group of hydroxymethyl EDOT totally reacted with succinic anhydride. The shift of methylene and methylene protons from 3.7-4.2 ppm in hydroxymethyl EDOT (peak b-d) to 3.9-4.3 ppm in EDOT-C4-COOH (peak b'-d') could be explained with the conversion of hydroxyl group to ester group.

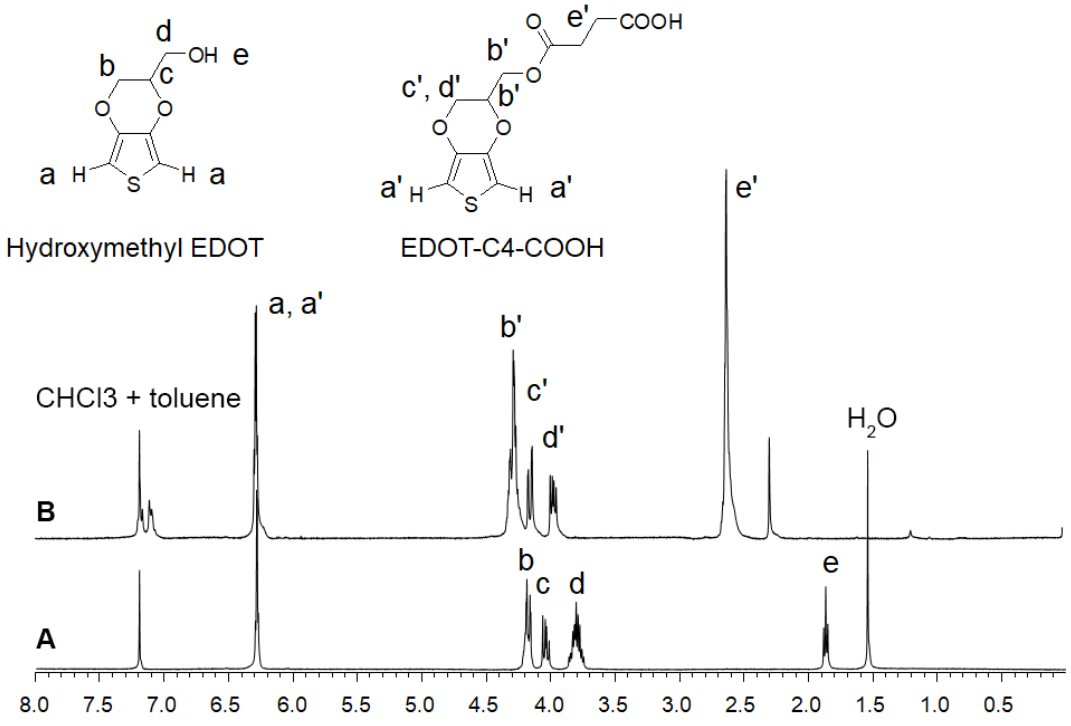

Figure 3.2 ^{1}H NMR spectra of (A) hydroxymethyl EDOT and (B) EDOT-C4-COOH.

In FT-IR spectra shown in **Figure 3.3**, hydroxymethyl EDOT exhibited aromatic C=C stretching peak at 1490 cm^{-1}, which was retained in EDOT-C4-COOH, suggesting that thiophene moiety remained intact after the reaction. Succinic anhydride, on the

other hand, showed 2 characteristic peaks of acid anhydride C=O stretching peaks at 1780 cm^{-1} (symmetric) and 1860 cm^{-1} (asymmetric), both of which did not appear in the FT-IR spectrum of the product, EDOT-C4-COOH. Instead, characteristic peaks of carbonyl group in ester at 1740 cm^{-1} and carboxylic acid at 1710 cm^{-1} emerged in the spectrum of EDOT-C4-COOH in roughly equal intensity, which confirmed that succinic anhydride was successfully reacted with hydroxymethyl EDOT.

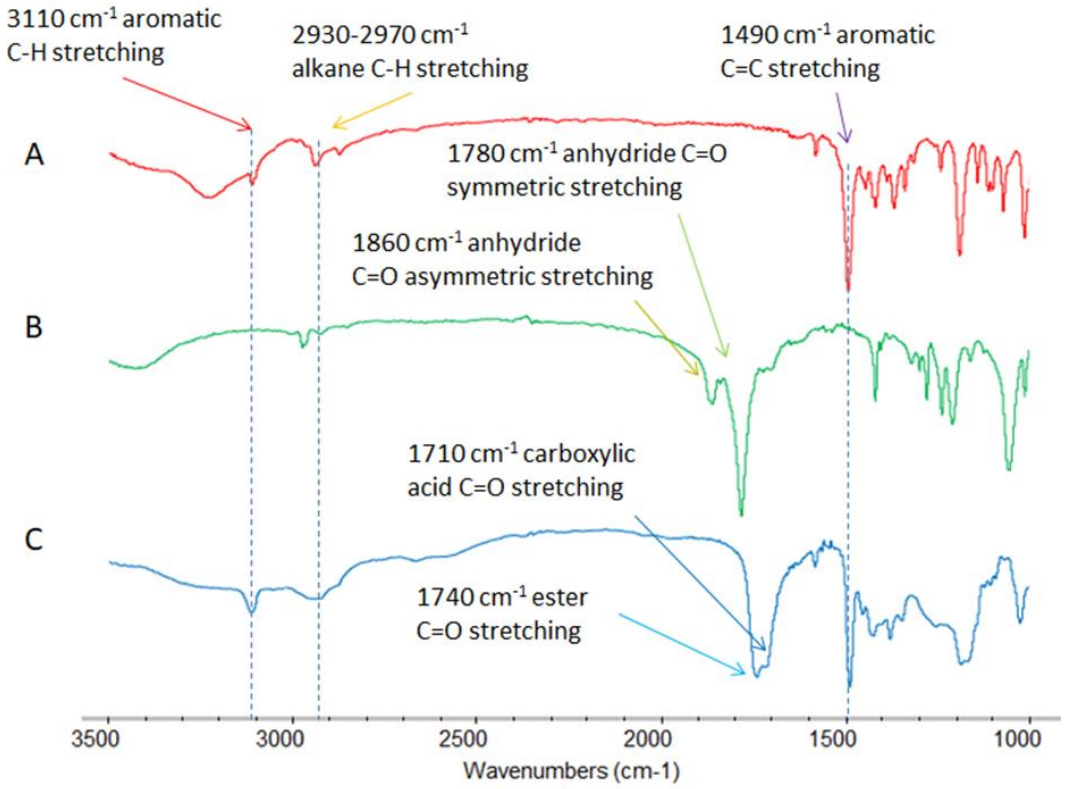

Figure 3.3 FT-IR spectra of (A) hydroxymethyl EDOT, (B) succinic anhydride, and (C) EDOT-C4-COOH.

3.1.3 Bromination of EDOT-C4-COOH

Unlike EDOT, bromination of EDOT-C4-COOH could not be performed using NBS. In general, in order to quench and remove NBS once the reaction was done, saturated $NaHCO_3$ solution would be used. This basic condition would deprotonate carboxyl group of both the reactant, EDOT-C4-COOH and the brominated product. To

circumvent this problem, pyridinium tribromide was chosen as an alternative brominating agent because the by-product formed, pyridinium bromide, could be removed using acidic HCl solution. The first attempt was to perform the reaction at room temperature. The color of the solution turned deep purple almost instantly, possibly due to quite high reactivity of the product, DBEDOT-C4-COOH towards polymerization. To prevent the premature polymerization in this bromination step, the reaction was performed at 0°C to decrease the possibility of early polymerization, which can be confirmed by the fact that the color of bromine disappeared rapidly during the bromination and the solution became colorless without turning purple, implying that no polymerization occurred.

Characterizations of the product, DBEDOT-C4-COOH, were performed by ^{1}H-NMR and FT-IR analysis. According to ^{1}H -NMR spectrum displayed in **Figure 3.4**, a decrease in intensity of the peak at 6.3 ppm, which can be assigned to hydroxymethyl EDOT's thiophene protons (peak a), confirmed that the majority of EDOT-C4-COOH was brominated. The percentage of conversion was calculated to be 92% by comparing integration of peak representing thiophene proton (peak a) with the peak corresponding to methylene protons of succinate moiety from both starting material and product (peak e and e') using the following equation:

$$\%conversion = \frac{\left(\left(\frac{E}{4}\right)-\left(\frac{A}{2}\right)\right)}{\left(\frac{E}{4}\right)} \times 100 \qquad \text{.....1}$$

in which A and E are the peak area of peak a and e', respectively. There was no attempt to fully brominate DBEDOT-C4-COOH due to the risk of premature polymerization and low amount of obtained product.

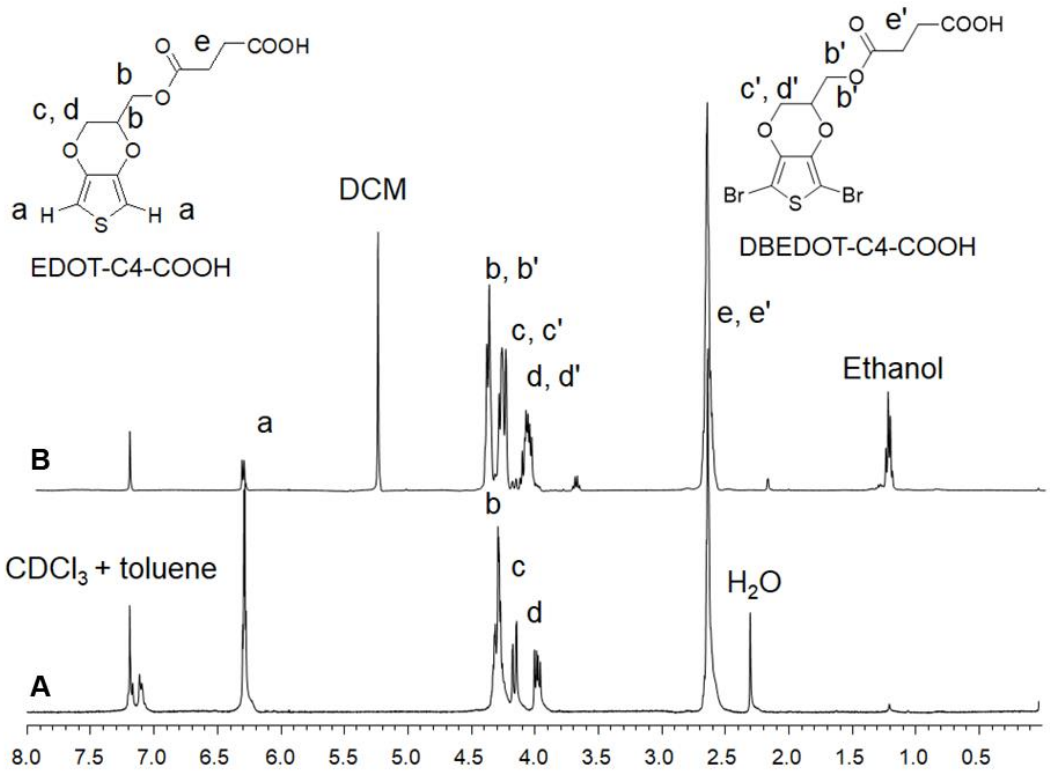

Figure 3.4 ^{1}H-NMR spectra of (A) hydroxymethyl EDOT and (B) EDOT-C4-COOH.

In FT-IR spectra, DBEDOT-C4-COOH still exhibited aromatic C=C stretching peak, albeit shifted to 1504 cm^{-1} due to the substitution of electron-withdrawing bromo groups, which was also confirmed through an absence of aromatic C-H stretching peak at 3110 cm^{-1}. Both characteristic peaks of carbonyl groups in ester at 1740 cm^{-1} and carboxylic acid at 1710 cm^{-1} remained intact, verifying that bromination did not affect the succinate ester moieties.

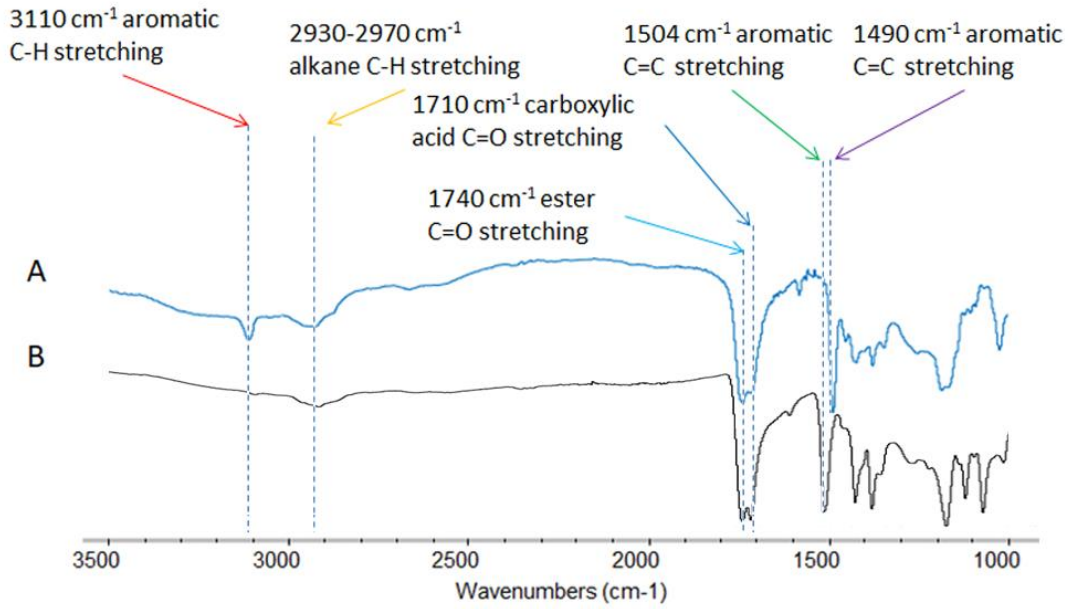

Figure 3.5 FT-IR spectra of (A) EDOT-C4-COOH and (B) DBEDOT-C4-COOH.

3.2 Preparation of Electrospun Fiber Mats

3.2.1 Poly(vinyl pyrrolidone)-Based Electrospun Fiber Mats

Poly(vinyl pyrrolidone) (PVP) was chosen as a polymer matrix for electrospinning due to its hydrophilicity, high melting point (150-180°C) as compared with the temperature required for solid state polymerization of EDOT (60-80°C), and its miscibility with a wide variety of solvents. Ethanol was found to be the best solvent for electrospinning, resulting in smooth fibers (**Figure 3.6A**) with a diameter of 829±173 nm using a PVP concentration of 10%(w/v). An addition of DBEDOT (1:1, w/w) to the polymer solution did not affect the overall morphology of the fiber mat even after heat-induced solid-state polymerization (**Figure 3.6B**), implying that DBEDOT did not affect the entanglement of polymer chain in the solution.

While the hydrophilicity of PVP could increase the contact between aqueous media and the electrode, its solubility in water would be detrimental to the usability of electrospun fiber mats, as it would be dissolved and collapse during the electrochemical process in aqueous solution and reduce the reproducibility of electrode. As PVP lacks of any functional group that could be used to perform the conventional covalent cross-linking, radical cross-linking initiated with ultraviolet (UV)

radiation was chosen. Hydrogen peroxide was added to the polymer solution as an initiator and the as-spun fiber mat was cross-linked under UV irradiation. The irradiated fiber was submerged in water for 24 hours to evaluate the effect of cross-linking. It was found that, even though the fibers would not be dissolved, they would greatly swell and lost their fibrous structure as can be seen in **Figure 3.6C**. This would render PVP unsuitable as polymer matrix to be used in aqueous media.

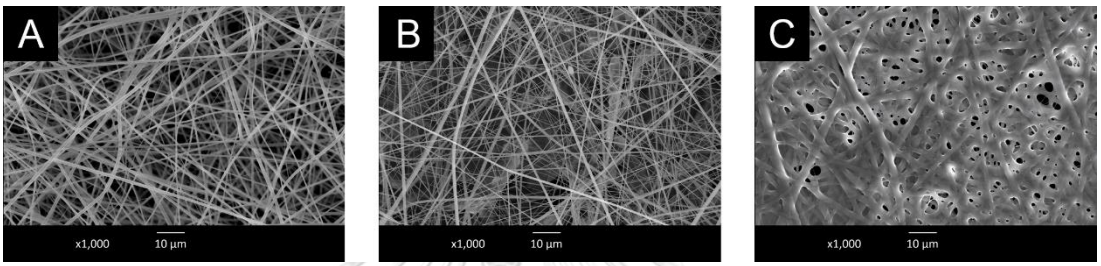

Figure 3.6 SEM micrographs of (A) electrospun PVP fiber mat, (B) PEDOT/PVP fiber mat, and (C) PEDOT/PVP fiber mat after UV crosslinking and immersion in water.

3.2.2 Poly(vinyl alcohol)-Based Electrospun Fiber Mats

3.2.2.1 Comparison between Conventional and Emulsion Electrospinning

Unlike PVP, poly(vinyl alcohol) (PVA) did not have a common solvent with DBEDOT that could be used in electrospinning. The only solvent that could dissolve both PVA and DBEDOT was dimethyl sulfoxide (DMSO), which was not suitable for electrospinning due to its high boiling point, hygroscopy, and lack of hydrogen bonding donor as compared with water, resulting in beads with no fibers formed after electrospinning DMSO solution of 15% PVA and DBEDOT (1:1, w/w) (**Figure 3.7**).

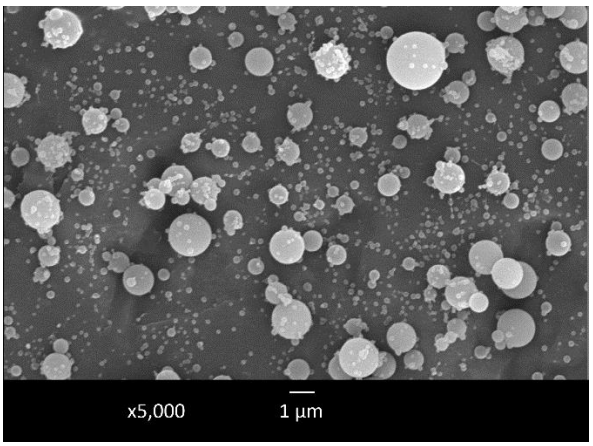

Figure 3.7 SEM micrographs of electrospun beads of PEDOT/PVA composite using DMSO as solvent.

To circumvent this problem, emulsion electrospinning technique was employed to fabricate the fiber mats. As compared with the PVA fiber mats electrospun from 12% w/v PVA in aqueous solution with a diameter of 212±28 nm (**Figure. 3.8a**), the fiber mat electrospun from 12% emulsion solution of PVA and DBEDOT (43% DBEDOT w/w) were shown to be beaded with increased average diameter to 547±82 nm (**Figure 3.8b**). The increase of fiber diameter was presumably from increase of solid content, while the large variation in the diameter was possibly due to unequal rate evaporation of organic phase containing DBEDOT and aqueous phase containing PVA, disrupting the uniformity of the fibers. An addition of silver nitrate as a precursor to form AgNPs resulted in a decrease of fiber diameter to 456±104 nm (**Figure 3.8c**). This may be explained as a result of an increased ionic strength of the solution from the addition of ionic salt causing stretching of electrun charged jet, thus yielded fibers with thinner diameter. [30-31] The overall morphology of the fibers, however, did not change.

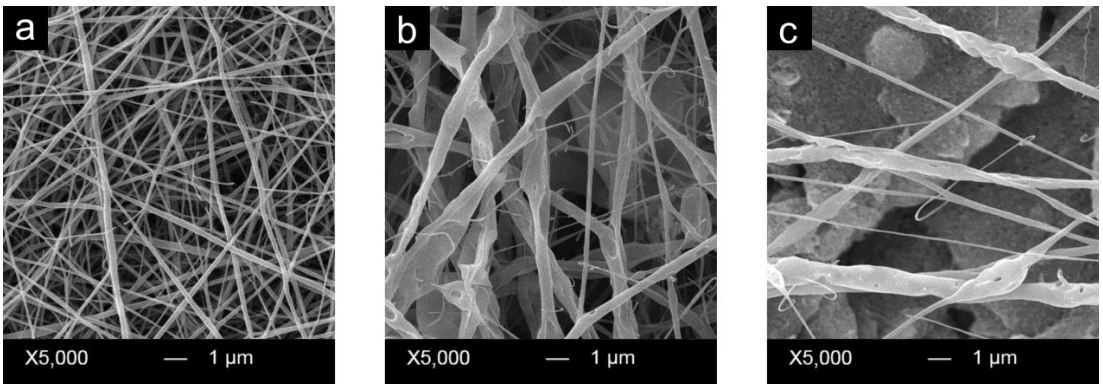

Figure 3.8 SEM micrographs of (a) electrospun PVA fiber mat, (b) PEDOT/PVA fiber mat deposited on aluminum foil, and (c) PEDOT/PVA/AgNPs fiber mat deposited on screen-printed carbon electrode.

As PVA is a water-soluble polymer, it must be cross-linked by glutaraldehyde to prevent the fiber from dissolving in aqueous media. The stability of the cross-linked fiber was investigated by immersing the cross-linked fiber in water for 24 hours. (**Figure 3.9**) As shown, the morphological features of the fibers remained the same as before the immersion, showing that the fibers remained stable in aqueous media.

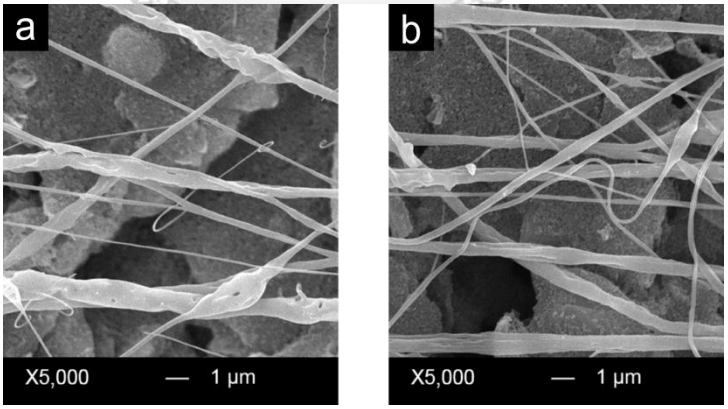

Figure 3.9 SEM micrographs of cross-linked electrospun PEDOT/PVA fiber deposited on screen-printed carbon electrode before (a) and after (b) immersion in water.

3.2.2.2 Characterization of Silver Nanoparticle in the Fiber Mats

The distribution of PEDOT and AgNPs in the electrospun PEDOT/PVA/AgNPs fiber mat was investigated by TEM. As depicted in **Figure 3.10**, AgNPs could be observed in the fiber as black particles with a size of 15±3 nm. PEDOT phase, meanwhile, seemed to spread evenly in the fiber without major separation, as seen with evenly dark color of the fiber compared to pale color of PVA/AgNPs fiber. This result implied that DBEDOT was properly dispersed in the PVA solution prior to the electrospinning.

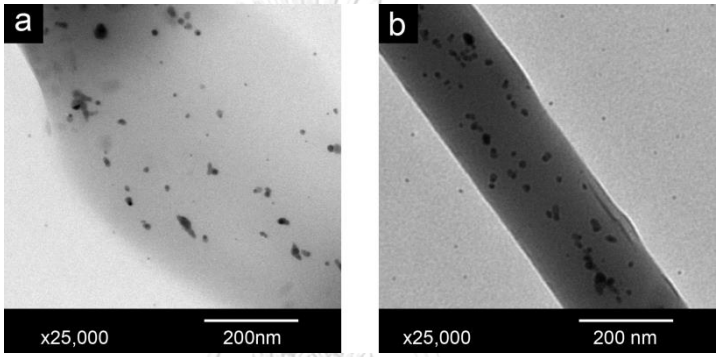

Figure 3.10 TEM micrographs of electrospun PEDOT/PVA fiber (a) and PEDOT/PVA/AgNPs fiber (b)

3.2.2.3 Thermogravimetric Analysis of Fiber Mats

Figure 3.11 shows the TGA thermograms of PEDOT/PVA fibers with and without AgNPs as compared with PEDOT and PVA. Thermal degradation profiles of PVA and PVA with AgNPs were very similar, both of which showed two major weight losses at 235-250°C and 364-480°C corresponding to dehydration reaction and fragmentation of PVA chains, respectively. The only difference was the amount of remaining ash, with PVA fiber with AgNPs having higher amount of ash due to the AgNPs being unable to decompose. For PEDOT, the major weight loss was observed at 110-210°C which could be the loss of molecular bromine dopant, and the minor weight lost was observed at 350-390°C. The thermal degradation profiles of PEDOT/PVA fibers with and without AgNPs showed major weight loss at 135-210°C, which is most likely the same weight loss of molecular bromine dopant as observed in the case of PEDOT. The slightly

higher initial temperature (135 vs 110 °C) may be ascribable to the entrapment by entangled polymeric chains of PVA so that it became more difficult for the molecular bromine to be degraded and released. Another major weight loss appears at 420-500°C corresponding to the fragmentation of polymer chain. Region between the major weight losses also showed a steady decline, which should be the combined results of dehydration reaction of PVA and loss of molecular bromine.

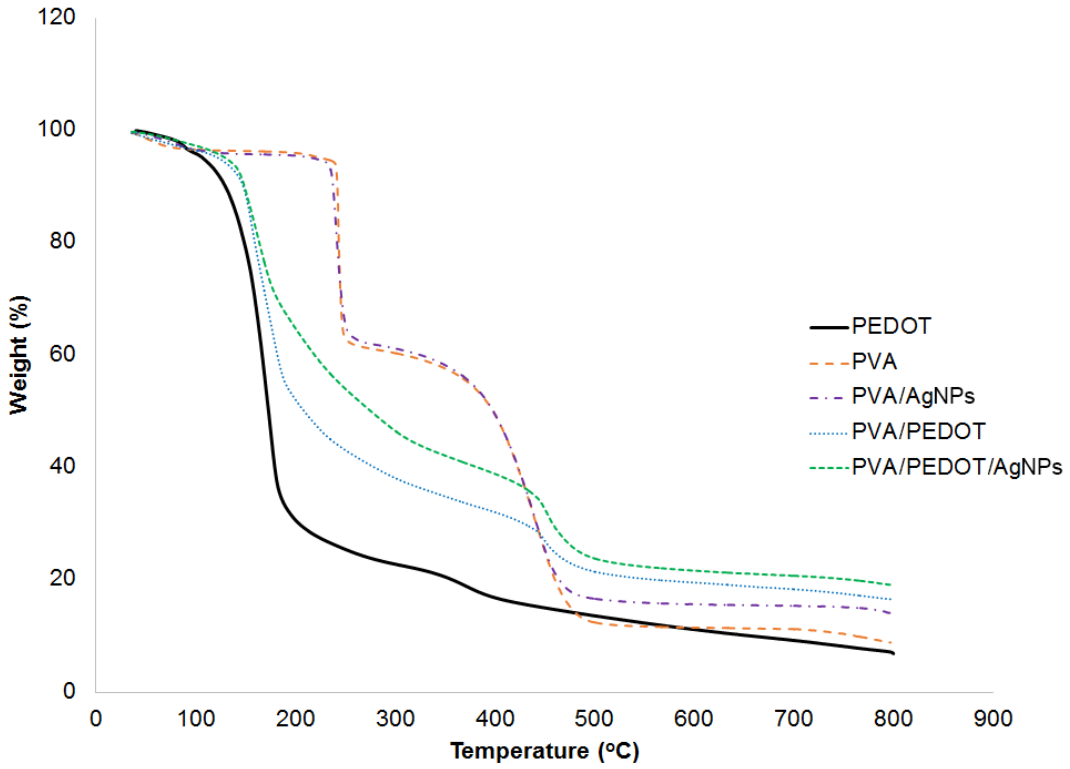

Figure 3.11 TGA thermograms of composite fibers

The calculated percentages of each component are shown in **Table 3.1**. While the calculated percentage of PVA and PEDOT in the fiber were both near the theoretical values, the percentage of AgNPs was 6 times higher than expected in both cases. This could be explained by the fact that the incorporated AgNPs exhibited lower melting temperature when compared with regular AgNPs which have melting point of 960°C.[32] At 150°C, far below the normal melting point, AgNPs could begin to

coalesce, forming network of particle that could trap the ash that should have decomposed, resulted in higher percentage than anticipated.

Table 3.1 Weight loss and calculated percentage of each phases of electrospun composite fibers

Sample	Ash (%)	PVA Portion (theory) (%)	PVA Portion (Exp.) (%)	PEDOT Portion (theory) (%)	PEDOT Portion (Exp.) (%)	AgNP (theory) (%)	AgNP (Exp.) (%)
PVA	9.40						
PVA/AgNPs	14.80	99.00	94.00			1.00	6.00
PEDOT	26.30						
PEDOT/PVA	16.80	57.00	56.30	43.00	43.70		
PEDOT/PVA /AgNPs	19.20	56.70	58.00	42.80	38.40	0.60	3.60

3.2.2.4 X-ray Photoelectron Spectroscopy (XPS) Analyses of Fiber Mats

Elemental composition and functional groups of electrospun fibers were analyzed by XPS. As expected, C1s and O1s dominated the atomic concentration at about 60% and 30%, respectively, in every electrospun fibers due to the majority of the matrix being PVA (**Table 3.2**). As shown in **Figure 3.12** and **Table 3.3**, the peak shape C1s suggested that there are several types of carbons in each composite. In all cases, deconvolution resulted in peaks that could be attributed to carbon that bonded only to hydrogen or carbon (C-H, C-C) and carbon that formed single bond with electronegative oxygen (C-O) because the structure of PVA consisted of methylene carbon atoms and carbon atoms bonded with hydroxy groups. Carbon that formed double bond with electronegative oxygen (C=O) was also presented in all samples due

to glutaraldehyde used in cross-linking and the decomposition of PVA backbone under x-ray irradiation during XPS analysis. Incidentally, atomic concentration of carbonyl carbon increased with addition of AgNPs generated *in situ*, which confirmed that AgNPs was formed through reduction of Ag^+ by the hydroxyl groups of PVA, resulted in the formation of oxidized PVA having carbonyl entities. In the case of the composite fiber with PEDOT-C4-COOH derivative and PEDOT (50%PEDOT-C4-COOH/PVA), there was a shoulder peak appearing at the highest binding energy implying that such carbon should bind with electronegative oxygen in the form of O-C=O.

Table 3.2 Atomic concentration of elements found in fibers (%)

Sample	C1s	O1s	S2p	Br3d	Ag3d
PVA	66.70	32.82	0.46	0.01	0.00
PVA/PEDOT	65.97	33.33	0.49	0.21	0.00
PVA/PEDOT/AgNPs	65.38	33.19	0.54	0.86	0.03
50%PEDOT-C4-COOH/PVA	64.13	33.92	1.92	0.02	0.00

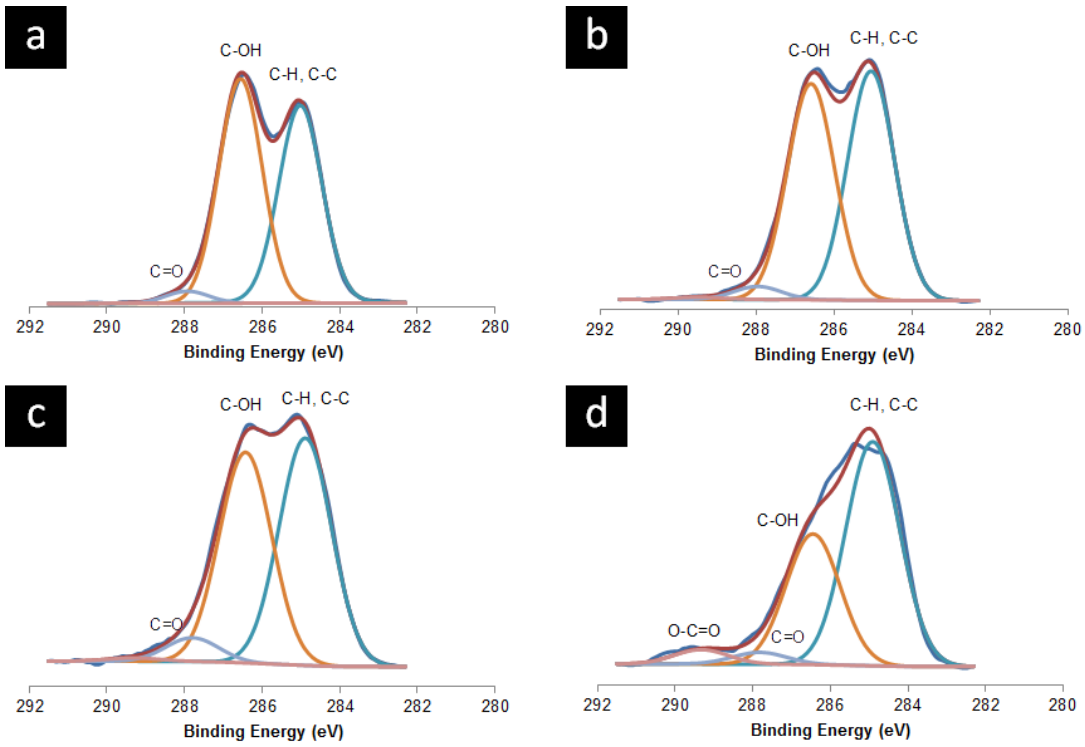

Figure 3.12 Deconvoluted C1s region of electrospun composite fibers as analyzed by XPS: (a) PVA, (b) PVA/PEDOT, (c) PVA/PEDOT/AgNPs, and (d) 50%PEDOT-C4-COOH/PVA.

Table 3.3 Atomic concentration of C atoms from deconvolution (%)

Sample	C-C,C-H (285 eV)	C-O (286.5 eV)	C=O (287.5 eV)	O-C=O (289 eV)
PVA	46.03	51.10	2.77	0.10
PEDOT/PVA	49.88	46.86	2.74	0.51
PEDOT/PVA/AgNPs	49.12	45.14	5.04	0.70
50%PEDOT-C4-COOH/PVA	58.63	34.38	3.12	3.88

As anticipated, the addition of PEDOT in the composite resulted in an appearance of S2p splitting into two major peaks (**Figure 3.13**): one that belongs to the thiophene units appear at lower binding energy (163-166 eV) than the other

onethat assigned to the sulfate group of SDS, the surfactant added to form emulsion. (**Table 3.4**) The addition of AgNPs resulted in an appearance of Ag3d peak which was splitted into 2 peaks ($Ag3d_{3/2}$ and $Ag3d_{5/2}$) (**Figure 3.13**). Small amount of bromine, the by-product of SSP was also found in both PEDOT/PVA and PEDOT/PVA/AgNPs composites (**Table 3.2**).

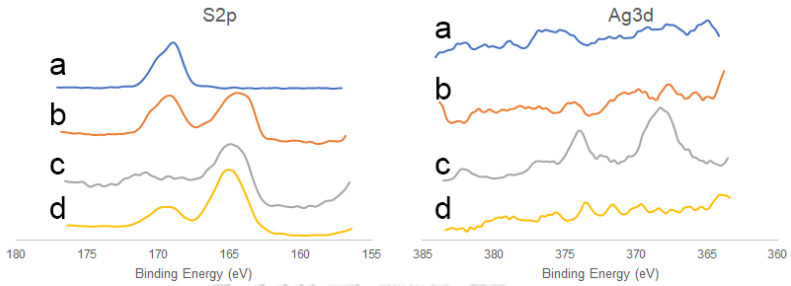

Figure 3.13 XPS narrow spectra of S2p and Ag3d regions of electrospun composite fibers: (a) PVA, (b) PVA/PEDOT, (c) PVA/PEDOT/AgNPs, and (d) 50%PEDOT-C4-COOH/PVA.

Table 3.4 Atomic concentration of S atoms from deconvolution (%)

Sample	thiophene (163-166 eV)	sulfate (169-170 eV)
PVA	0.83	99.17
PEDOT/PVA	56.31	43.69
PEDOT/PVA/AgNPs	75.35	24.65
50%PEDOT-C4-COOH/PVA	75.16	24.84

3.3 Electrochemical Analyses of Electrodes modified by Electrospun Fibers

3.3.1 Cyclic Voltammetry

3.3.1.1 Effect of Material in the Composite

To investigate the effect of the material variation on the electrochemical signals, the newly developed PEDOT/PVA fiber-modified electrodes were analyzed by cyclic voltammetry (CV) using a standard $[Fe(CN)_6]^{3-}/[Fe(CN)_6]^{4-}$ redox couple in comparison with PVA fiber-modified electrodes and unmodified screen-printed carbon electrodes. As demonstrated in **Figure 3.14-3.15**, the PVA fiber-modified electrode yielded low background current with the current response being almost equal to the unmodified electrode, while the PEDOT/PVA fiber-modified electrode yielded significantly increased current response. These results showed that the PVA fiber could reduce the charge accumulation and the addition of PEDOT facilitated the electron transfer process. Furthermore, introduction of AgNPs or carboxylic group in the form of PEDOT-C4-COOH to the electrospun fibers seemed to further increase the current response in both cases. The addition of conductive AgNPs could further facilitate the electron transfer process, albeit in small extent due to only a small amount of incorporated AgNPs (1% w/w). As for the addition of PEDOT-C4-COOH, some of the carboxylic groups would dissociate and became carboxylate ion, thus increase swelling of the fiber in the solution, allowing the reactive species ($[Fe(CN)_6]^{3-}/[Fe(CN)_6]^{4-}$ redox couple) to further interact with the electrode.

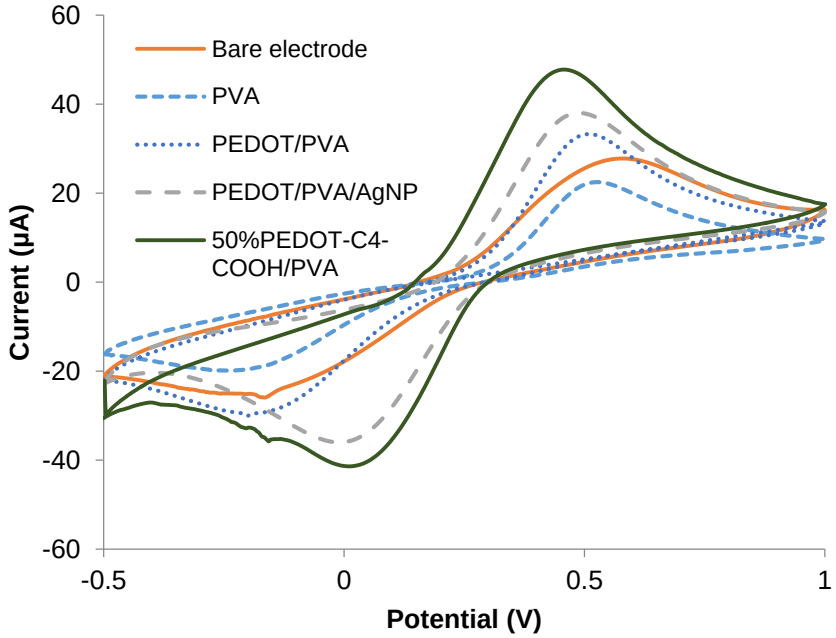

Figure 3.14 Cyclic voltammograms of electrodes modified by electrospun fibers

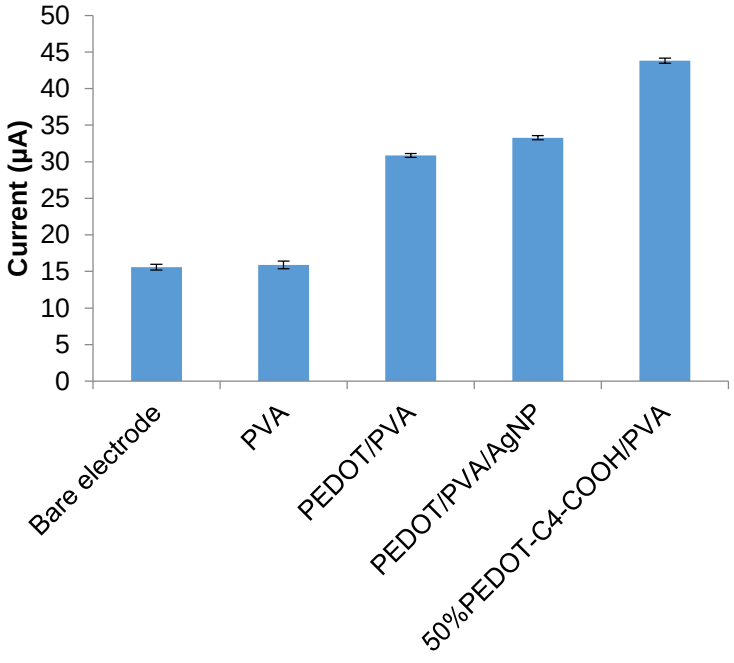

Figure 3.15 Current intensity measured from cyclic voltammograms of electrodes modified by electrospun fibers.

3.3.1.2 Effect of the Thickness of Fiber Mats

The relation between fiber thickness and electrochemical signal was then investigated by using CV to monitor the electron transfer process in the modified electrodes using a standard $[Fe(CN)_6]^{3-}/[Fe(CN)_6]^{4-}$ redox couple (**Figure 3.16**). The fiber with thickness of 4.8 μm yielded the highest current response (**Figure 3.17**). Further increase in fiber thickness resulted in a decrease of current response and an increase in background signal. The decrease of response could be the result of non-conductive PVA layer hindering the electron transfer process.

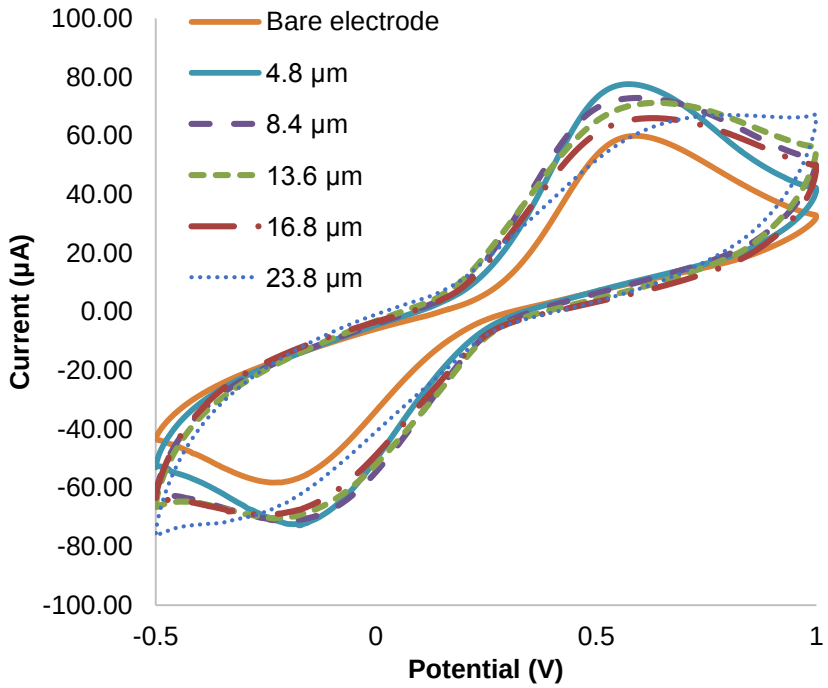

Figure 3.16 Cyclic voltammograms of 0.1 M standard $[Fe(CN)_6]^{3-}/[Fe(CN)_6]^{4-}$ solution performed on the electrodes modified by PEDOT/PVA electrospun fiber mats having varied thickness.

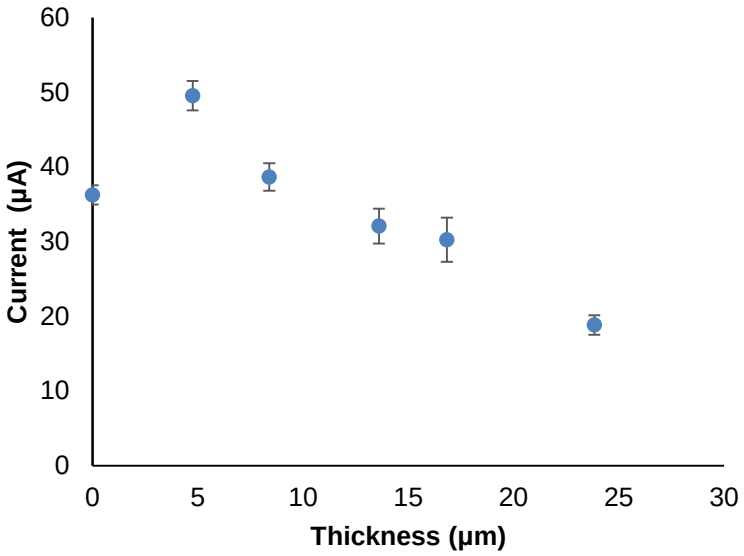

Figure 3.17 Plot between thickness of the fiber mat and electrochemical signal

3.3.2 Square-Wave Anodic Stripping voltammetry (SWASV)

To evaluate the potential of PEDOT/PVA fiber-modfified electrode for electrochemical application, SWASV was used to detect Zn(II), Cd(II), and Pb(II) due to its high sensitivity and good linear range. Anodic peak potentials for Zn(II), Cd(II), and Pb(II) were measured at -0.97, -0.71, and -0.49 V, respectively (**Figure 3.18**). While the anodic peak of Cd(II) and Pb(II) were readily detected, the peak of Zn(II) had very weak intensity. In order to improve the detection of Zn(II), AgNPs were added to the PVA matrix in order to increase the deposition of Zn due to silver's affinity to zinc allowed AgNPs to act as nucleation site for Zn deposition [33-35]. As shown in **Figure 3.19**, the current intensity of Zn(II) anodic peak increases from 0.80±0.11 to 4.75±0.44 µA, almost 6 times of that obtained from the electrode without AgNPs. The anodic peak of Cd(II) and Pb(II), however, remained almost unaltered. Unlike Ag-Zn alloy, which have negative Gibbs free energy of mixing, Ag-Pb and Ag-Cd alloys have positive Gibbs free energy of mixing, which could be the reason why Ag assists in the deposition of Zn but not Pb and Cd. [36]

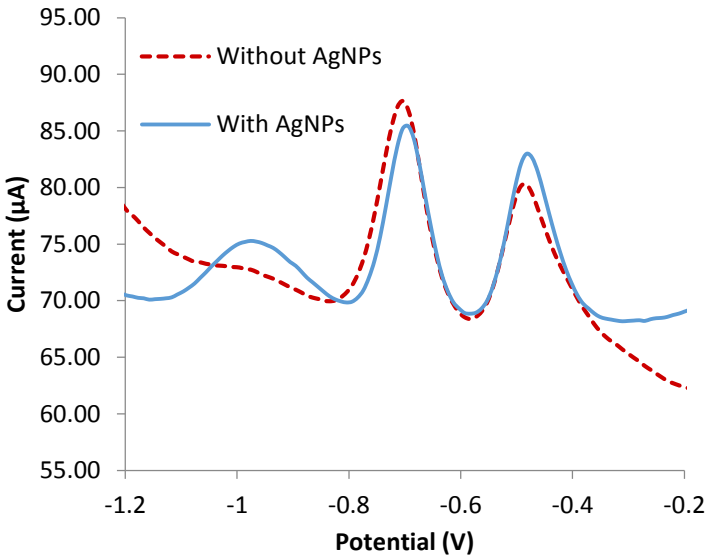

Figure 3.18 Voltammograms of Zn(II), Cd(II), and Pb(II) with concentration at 80 ppb from SWASV using PEDOT/PVA fiber-modified electrode with and without AgNPs.

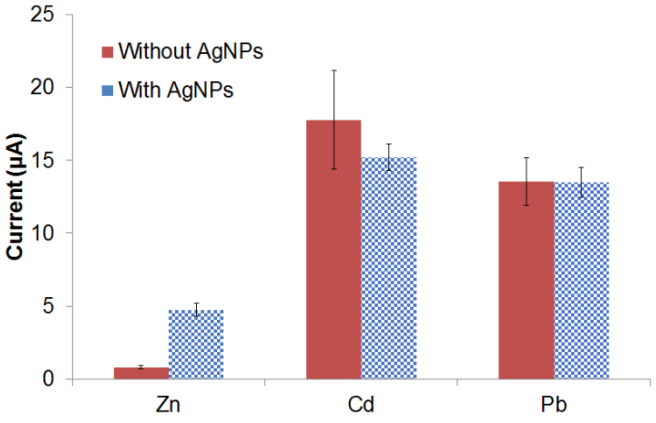

Figure 3.19 Current intensity of Zn(II), Cd(II), and Pb(II) obtained from SWASV analysis using PEDOT/PVA fiber-modified electrode with and without AgNPs.

Anodic peak currents of the three metals using PEDOT/PVA/AgNPs fibers-modified electrodes and the resulting calibration plots are shown in **Figure 3.20** and **3.21**, respectively. The calibration plots were linear over a range from 1.0 to 80 ppb with correlation coefficients exceeding 0.9900 for all metals. The experimentally determined limits of detection (LODs) for the system evaluated were 31 ppb for Zn(II),

16 ppb for Cd(II) and 12 ppb for Pb(II) based on signal-to-noise ratios for peak height of three (S/N = 3).

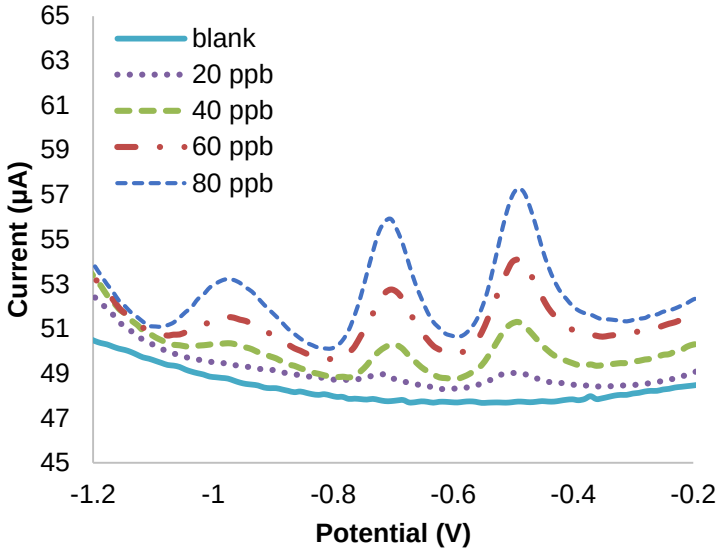

Figure 3.20 Voltammograms of Zn(II), Cd(II), and Pb(II) with various concentration obtained from SWASV analysis using PEDOT/PVA/AgNPs fibers- modified electrode.

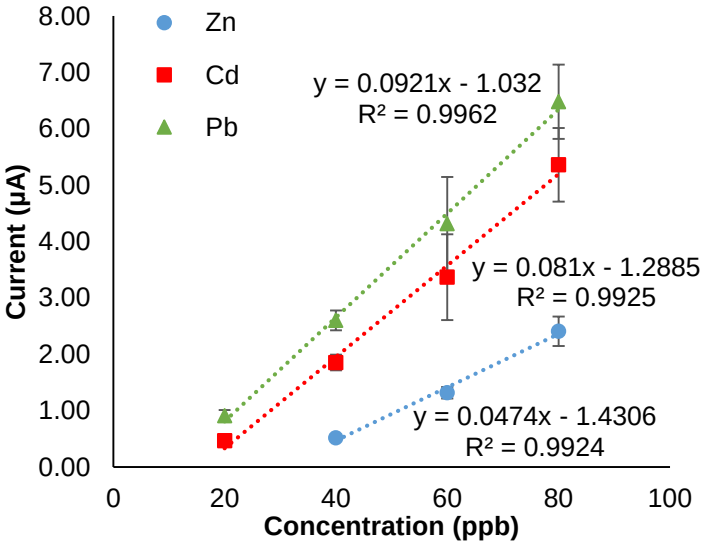

Figure 3.21 Calibration plots of signal currents of Zn(II), Cd(II), and Pb(II) with various concentration obtained from SWASV analysis using PEDOT/PVA/AgNPs fibers-modified electrode

To increase electrode sensitivity, Bismuth ion (Bi(III)) was used to form a metal-Bi alloy on the electrode surface to facilitate the process of nucleation during metal ion deposition [37-39]. Anodic peak currents of the three metals after addition of Bi and the resulting calibration plots are shown in **Figure 3.22** and **3.23**, respectively. The enhancement of signal was obvious, with an increase of signal from Cd(II) and Pb(II) ions with lower LODs (7 ppb and 8 ppb, respectively) and slopes of the calibration plots was double from those without Bi. Signal of Zn(II), on the other hand, received little benefit from the Bi(III) addition. The signal could be detected at lower concentration than that without Bi (LOD = 11 ppb) but the increase of signal was not as apparent with Cd(II) and Pb(II). The result could be explained by the fact that Zn(II) has more affinity to Ag than Bi. As such, the addition of Bi(III), while still increases the signal of Zn, would not possess a strong influence as found on the signals of Cd(II) and Pb(II).

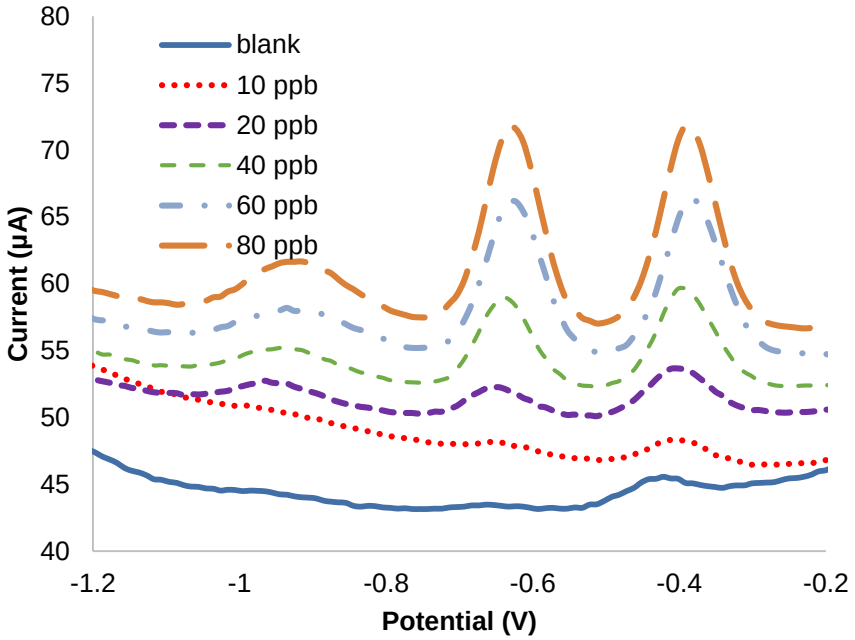

Figure 3.22 Voltammograms of Zn(II), Cd(II), and Pb(II) with various concentration obtained from SWASV analysis using PEDOT/PVA/AgNPs fibers-modified electrode with the addition of 300 ppb Bi(III).

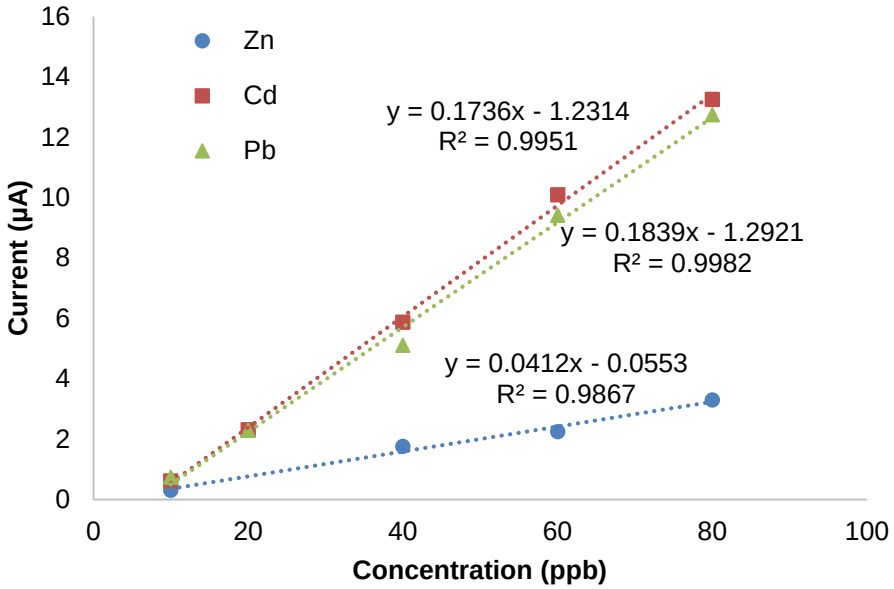

Figure 3.23 Calibration plots of signal currents of Zn(II), Cd(II), and Pb(II) with various concentrations obtained from SWASV analysis using PEDOT/PVA/AgNPs fibers-modified electrode with the addition of 300 ppb Bi(III).

The electrospun fiber of 50%PEDOT-C4-COOH/PVA was also evaluated for its potential enhancement in metal detection. Anodic peak currents of the three metals after the addition of Bi and the resulting calibration plots are shown in **Figure 3.24** and **3.25**, respectively. As expected, without an enhancement from AgNPs, the anodic peak of Zn(II) was low in all concentrations, resulting in relatively high LOD (26 ppb). In the case of Cd(II) and Pb(II), however, the peak heights increased greatly, resulting in lower LOD (5.9 ppb and 1.5 ppb, respectively) and the slopes of the calibration plots were greater than when using Bi(III) ion alone. The result could be explained by the attraction between carboxylate ion of PEDOT-C4-COOH and metal ions that facilitates the deposition of metal ions onto the surface, which, in turn, increases the anodic current in the stripping step. It might be possible to combine the effect of both carboxylic group and AgNPs to further increase the detection capability of the fiber-modified electrode in the future.

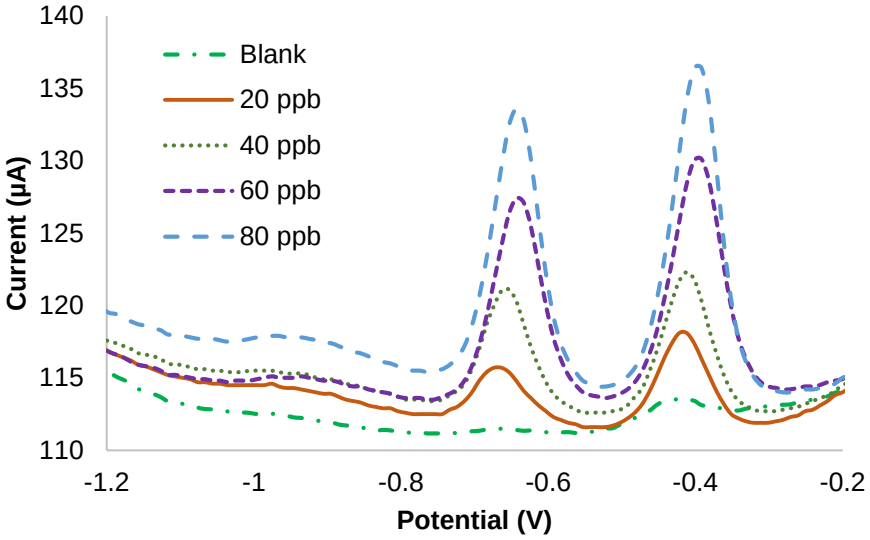

Figure 3.24 Voltammograms of Zn(II), Cd(II), and Pb(II) with various concentration from SWASV using electrode modified with PEDOT-C4-COOH/PVA fibers with the addition of 300 ppb Bi(III).

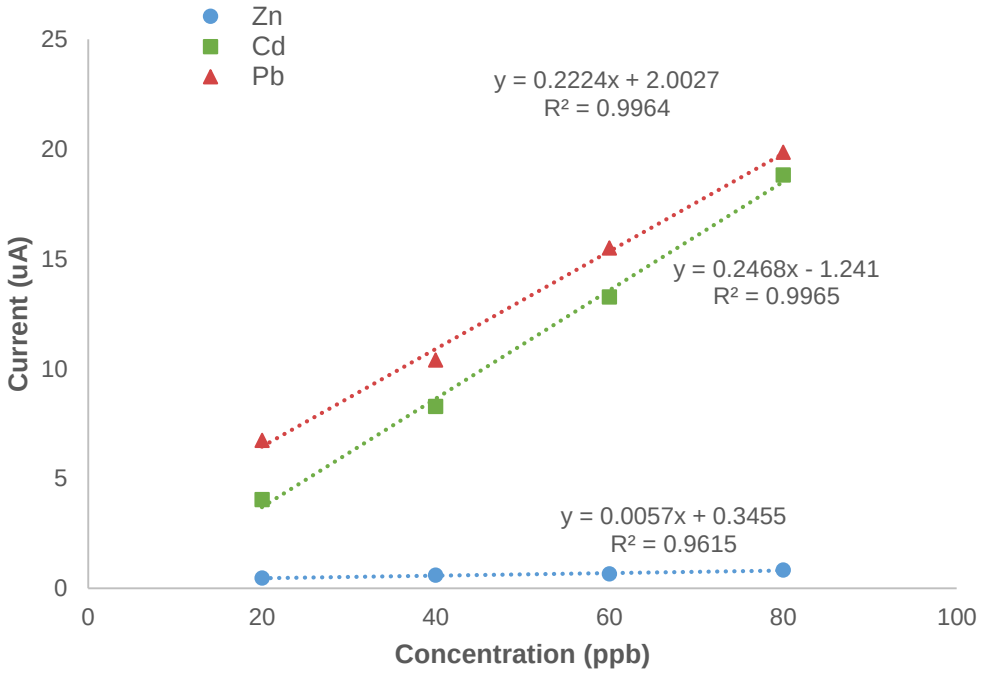

Figure 3.25 Calibration plots of signal currents of Zn(II), Cd(II), and Pb(II) with various concentration obtained from SWASV analysis using PEDOT-C4-COOH/PVA fibers-modified electrode with the addition of 300 ppb Bi(III).

Electrochemical performance of the PEDOT/PVA/Ag fiber-modified electrode was compared with similar systems in the literature for measuring Zn(II), Cd(II), and Pb(II) (**Table 3.5**). Although the LOD presented in this work is comparable to other reports, it is achieved through a simple process with commercially available polymer (PVA) and it is also the first time that solid state polymerized PEDOT was used in electrochemical analysis. Analysis of real sample, however, would still require further optimization in order to provide reproducible results.

Table 3.5 Limit of detection in ppb of Zn(II), Cd(II), and Pb(II) obtained from SWASV analysis using composite fiber-modified electrode as compared with other types of electrodes.

Electrode	Zn(II)	Cd(II)	Pb(II)	Reference
PEDOT/PVA/AgNPs	31	16	12	This work
PEDOT/PVA/AgNPs + Bi(III)	11	7	8	This work
50%PEDOT-C4-COOH/PVA+ Bi(III)	26	5.9	1.5	This work
Carbon/BiNPs	4.9	1.7	1.3	[37]
screen-printed carbon nanotubes	11	0.8	0.2	[40]
N-doped microporous carbon/Nafion/bismuth	-	1.5	0.05	[41]
PEDOT/SDS on glassy carbon	25	5	20	[42]
EPA regulation	5000	5	15	[43], [44]

3.4 Attempt in Modification of Electrospun Fibers with Enzyme

To test the applicability of the 50%PEDOT-C4-COOH/PVA fiber-modified electrode in immobilization of biomolecular probes, enzyme glucose oxidase (GOx) was used as a model. After immobilization of GOx using EDC/NHS coupling reagent, the fiber-modified electrode was characterized by ATR-FTIR and EIS analysis. The FTIR spectra (**Figure 3.26**) showed no noticeable difference between that of the fiber before and after modification, while EIS Nyquist plot (**Figure 3.27**) showed great change in charge transfer resistance (R_{ct}, the inset). The result implied that there could be some enzyme attached on the fibers' surface which would increase the R_{ct}, the amount of enzyme may however be too low to be detected by FTIR.

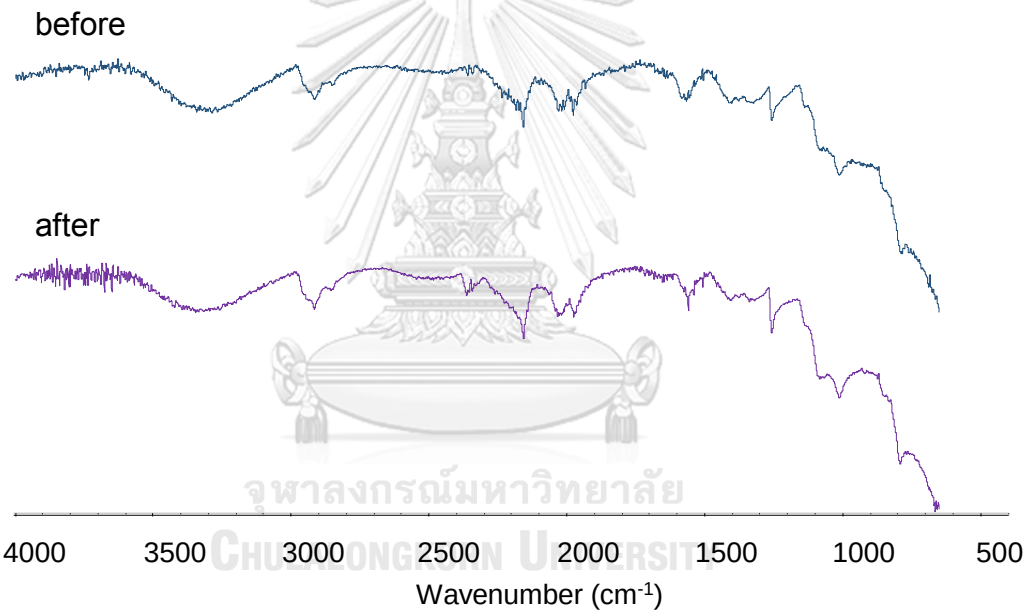

Figure 3.26 ATR-FTIR spectra of PEDOT-C4-COOH/PVA fibers-modified electrode before and after GOx immobilization.

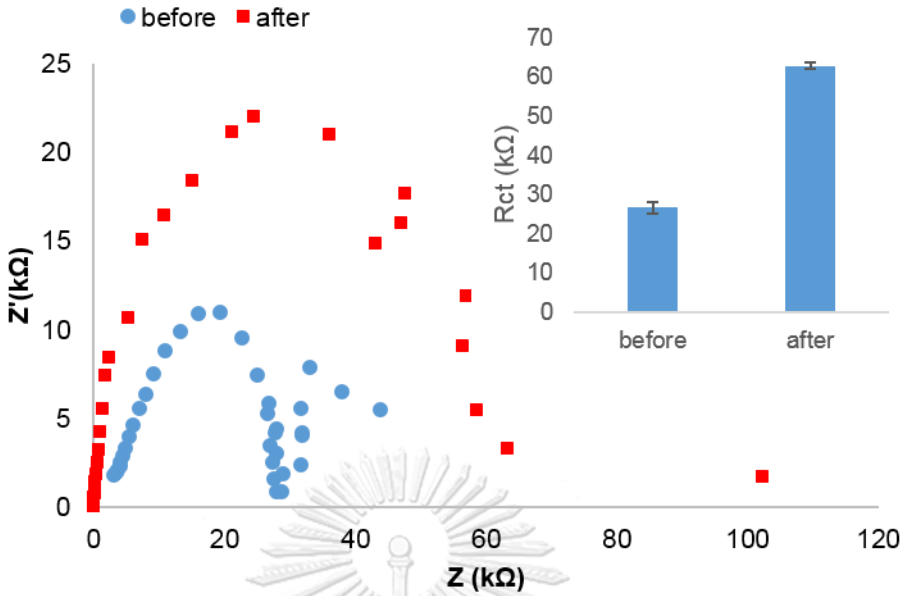

Figure 3.27 The Nyquist plot of EIS of PEDOT-C4-COOH/PjVA fibers-modified electrode before and after GOx immobilization. The inset showed R_{ct} calculated from the Nyquist plot.

To optimize the condition for the detection, amperometry of phosphate buffer solution before and after an addition of hydrogen peroxide was performed in a range of -1.0V to 1.0V. From the relationship plot between amperogram signal and the potential (**Figure 3.28a**) and plot between signal to background ratio and the potential (**Figure 3.28b**), the potential of -0.7 V was chosen for its high current and acceptable signal to background ratio. The calibration curve between signal current and the concentration of hydrogen peroxide is shown in **Figure 3.29**, with a linear range of 0-22 mM. At higher concentration, the slope of calibration curve greatly decreased and R^2 became lower than 0.99, rendered it unsuitable to be used as a standard.

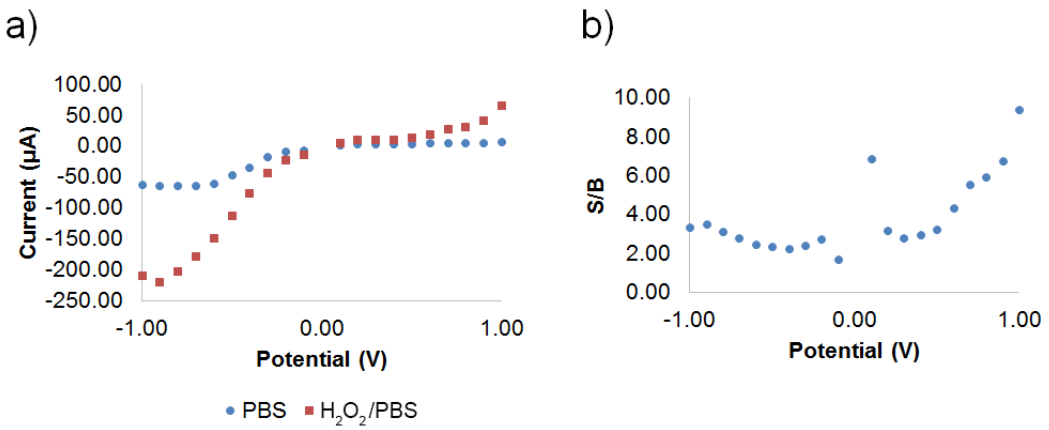

Figure 3.28 The relationship plot between signal current (a) or signal to background ratio (b) and the potential obtained from the amperogram of 0.1 mM PBS and 30 mM hydrogen peroxide in 0.1 mM PBS.

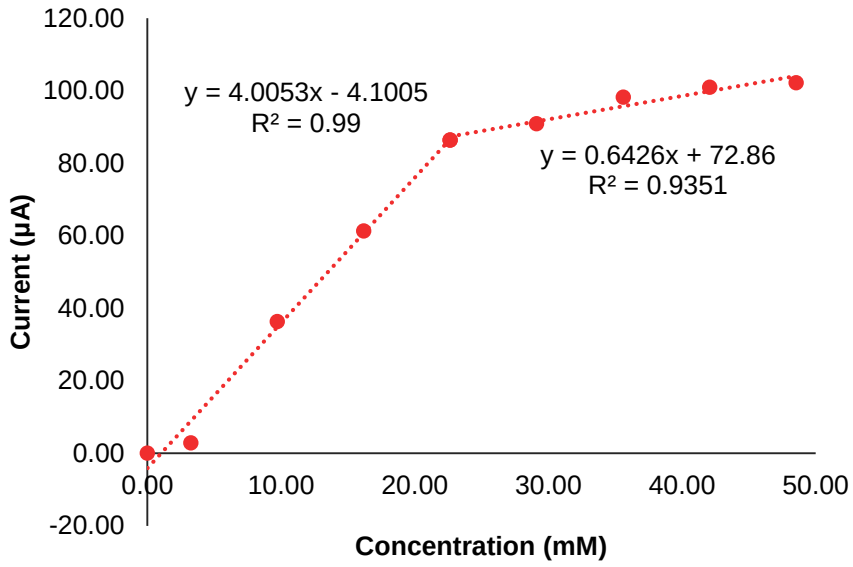

Figure 3.29 Calibration curve of signal current and concentration of hydrogen peroxide in 0.1 mM PBS obtained from amperometry.

Despite the good detection of hydrogen peroxide, an addition of 0.1 mM glucose caused the decrease in signal instead of expected increase (**Figure 3.30**). While the decrease could be explained by decrease of ion mobility due to increase of nonionic species, this outcome suggested that the addition of glucose did not result

in electrochemical signal as expected. In order to discern whether the lack of signal was due to lack of active enzyme on the surface or that the enzyme was already inactive, 10 µL 1 mg/mL GOx solution was added to the solution. The increase of signal observed made it certain that while some of the enzyme was attached to the surface as seen from EIS, the amount was not enough to act as probe for the glucose analysis. It was possible that the amount of carboxylic group in the 50%PEDOT-C4-COOH/PVA fibers was not enough to immobilize GOx for the analysis. In order to solve this problem, the conductive polymer part in the electrospun composite fiber might have to be prepared from 100%DBEDOT-C4-COOH without the addition of DBEDOT.

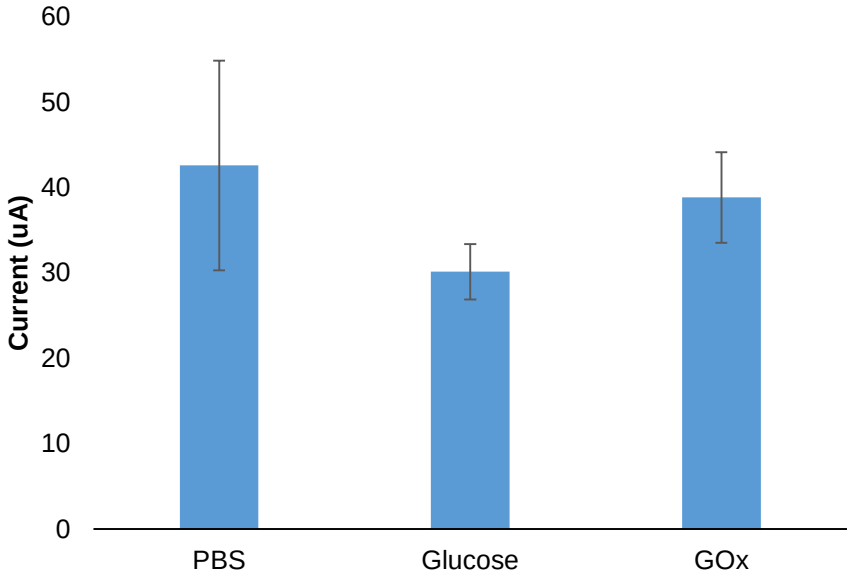

Figure 3.30 Electrochemical signal obtained from 0.1 mM PBS as compared with those with the addition of glucose and GOx using amperometry.

Chapter IV

CONCLUSION AND SUGGESTIONS

Solid monomers, namely DBEDOT and DBEDOT-C4-COOH were successfully synthesized by bromination of EDOT and EDOT-C4-COOH, respectively as verified by 1H NMR and FT-IR spectroscopy. While DBEDOT was successfully synthesized at ambient temperature, DBEDOT-C4-COOH had to be synthesized at 0°C in order to prevent premature oxidative polymerization of EDOT-C4-COOH.

Initially, PVP seemed to be a promising polymer matrix for electrospinning due to good common solvent with DBEDOT and excellent quality of electrospun fiber mats, however, its water solubility and lacking of reactive functional group towards conventional cross-linking made it impractical for the application in aqueous media. As for PVA, the only solvent that could dissolve both PVA and DBEDOT was dimethyl sulfoxide (DMSO), which was not suitable for electrospinning. Emulsion electrospinning technique was then employed to fabricate the fiber mats by using an emulsion of PVA solution and DBEDOT solution. As compared with the electrospun PVA fibers with the diameter of 212±28 nm, the electrospun PEDOT/PVA fibers had larger diameter of 547±82 nm and less uniform morphology. The addition of AgNPs generated *in situ* reduced the diameter of the electrospun PEDOT/PVA fibers down to 456±104 nm, with the unchanged morphology. The cross-linking of the fibers with glutaraldehyde vapor was successful as verified by the fiber morphology was preserved after immersion in water for 24 hours.

Electrospun PEDOT/PVA, PEDOT/PVA/AgNPs, and 50%PEDOT-C4-COOH/PVA composite fibers were successfully fabricated. Composition of the fibers calculated from TGA data was close to the theoretical value. In the case of PEDOT/PVA/AgNPs fibers, the presence and distribution of AgNPs was confirmed by TEM, in which AgNPs was found as black particles spreading inside the fibers, and XPS, via the appearance of Ag3d peaks. As for the 50%PEDOT-C4-COOH/PVA fibers, the presence of carboxylic group was confirmed by the emergence of O-C=O peak upon C1s peak deconvolution.

The PEDOT/PVA fiber-modified electrodes were characterized by cyclic voltammetry (CV) using a standard $[Fe(CN)_6]^{3-/4-}$ redox couple in comparison with the PVA fiber-modified electrodes and unmodified screen-printed carbon electrodes. The PEDOT/PVA fiber-modified electrode yielded significantly increased current response. Introduction of AgNPs or PEDOT-C4-COOH to the electrospun fibers seemed to further increase the current response in both cases. The fiber thickness was optimized to be 4.8 μm.

PEDOT/PVA fiber-modfified electrode was evalutated for its potential in electrochemical application. First, simultaneous detection of Zn(II), Cd(II), and Pb(II) was performed using SWASV technique. While the anodic peak of Cd(II) and Pb(II) were readily detected, the peak of Zn(II) had very weak intensity. Addition of AgNPs greatly enhanced the current intensity of Zn(II) anodic peak whereas the anodic peaks of Cd(II) and Pb(II) remained almost the same. The experimentally determined limits of detection (LODs) for the system evaluated were 31 ppb for Zn(II), 16 ppb for Cd(II) and 12 ppb for Pb(II). Addition of Bi(III) resulted in major enhancement, with lower LOD of 11 ppb for Zn(II), 7 ppb for Cd(II) and 8 ppb for Pb(II). The electrospun fibers of 50%PEDOT-C4-COOH/PVA was also evaluated in efficiency improvement of metal detection. While Cd(II) and Pb(II) had increased peak height and lower LOD (5.9 ppb and 1.5 ppb, respectively) the anodic peak of Zn(II) was low in all concentrations with LOD of 26 ppb. To further improve the detection capability of the fiber-modified electrode, a combination of both carboxylic group and AgNPs is proposed as a future route to develop the fiber-modified electrode.

50%PEDOT-C4-COOH/PVA fiber-modified electrode was evalutated for its capability in immobilization of biomolecular probes using enzyme glucose oxidase (GOx) as a model. Despite the supposed presence of GOx as implied by EIS analysis and the good detection capability for hydrogen peroxide, the electrode produced no response from glucose. Addition of GOx confirmed the activity of the enzyme, which suggested that the amount of GOx was not enough to act as probe for the glucose analysis. It was possible that the amount of carboxylic group in the 50%PEDOT-C4-COOH/PVA fibers was not enough to significantly immobilize GOx for the analysis. In

order to solve this problem, the conductive polymer part in the electrospun composite fiber might have to be prepared from 100%DBEDOT-C4-COOH without the addition of DBEDOT.

REFERENCES

[1] Stenger-Smith, J. D., Intrinsically Electrically Conducting Polymers. Synthesis, Characterization, and Their Applications. *Progress in Polymer Science* **1998,** *23*, 57-79.

[2] Hoeben, F. J. M.; Jonkheijm, P.; Meijer, E. W.; Schenning, A. P. H. J., About Supramolecular Assemblies of **TT**-Conjugated Systems. *Chemical Reviews* **2005,** *105*, 1491-1546.

[3] Jonas, F.; Schrader, L., Conductive Modifications of Polymers with Polypyrroles and Polythiophenes. *Synthetic Metals* **1991,** *41*, 831-836.

[4] Aasmundtveit, K. E.; Samuelsen, E. J.; Inganäs, O.; Pettersson, L. A. A.; Johansson, T.; Ferrer, S., Structural aspects of electrochemical doping and dedoping of poly(3,4-ethylenedioxythiophene). *Synthetic Metals* **2000,** *113*, 93-97.

[5] King, Z. A.; Shaw, C. M.; Spanninga, S. A.; Martin, D. C., Structural, chemical and electrochemical characterization of poly(3,4-Ethylenedioxythiophene) (PEDOT) prepared with various counter-ions and heat treatments. *Polymer* **2011,** *52*, 1302-1308.

[6] Groenendaal, L.; Jonas, F.; Freitag, D.; Pielartzik, H.; Reynolds, J. R., Poly(3,4-ethylenedioxythiophene) and Its Derivatives: Past, Present, and Future. *Advanced Materials* **2000,** *12*, 481-494.

[7] Balint, R.; Cassidy, N. J.; Cartmell, S. H., Conductive Polymers: Towards a Smart Biomaterial for Tissue Engineering. *Acta Biomaterialia* **2014,** *10*, 2341-2353.

[8] Meng, H.; Perepichka, D. F.; Bendikov, M.; Wudl, F.; Pan, G. Z.; Yu, W.; Dong, W.; Brown, S., Solid-State Synthesis of a Conducting Polythiophene via an Unprecedented Heterocyclic Coupling Reaction. *Journal of the American Chemical Society* **2003,** *125*, 15151-15162.

[9] Meng, H.; Perepichka, D. F.; Wudl, F., Facile Solid-State Synthesis of Highly Conducting Poly(ethylenedioxythiophene). *Angewandte Chemie International Edition* **2003,** *42*, 658-661.

[10] Yin, X.; Wu, F.; Fu, N.; Han, J.; Chen, D.; Xu, P.; He, M.; Lin, Y., Facile Synthesis of Poly(3,4-ethylenedioxythiophene) Film via Solid-State Polymerization as High-Performance Pt-Free Counter Electrodes for Plastic Dye-Sensitized Solar Cells. *ACS Applied Materials & Interfaces* **2013,** *5*, 8423-8429.

[11] McGraw, M.; Kolla, P.; Yao, B.; Cook, R.; Quiao, Q.; Wu, J.; Smirnova, A., One-step solid-state in-situ thermal polymerization of silicon-PEDOT nanocomposites for the application in lithium-ion battery anodes. *Polymer* **2016,** *99*, 488-495.

[12] Yan, B.; Matsushita, S.; Akagi, K., Aligned carbon and graphite fibers prepared from poly(3,4-ethylenedioxythiophene) single crystals synthesized by solid-state polymerization and their supercapacitor performance. *Journal of Materials Chemistry C* **2017,** *5*, 3823-3829.

[13] Pisuchpen, T.; Keaw-on, N.; Kitikulvarakorn, K.; Kusonsong, S.; Sritana-anant, Y.; Supaphol, P.; Hoven, V. P., Electrospinning and solid state polymerization: A simple and versatile route to conducting PEDOT composite films. *European Polymer Journal* **2017,** *96*, 452-462.

[14] Zhang, L.; Wen, Y.; Yao, Y.; Xu, J.; Duan, X.; Zhang, G., Synthesis and Characterization of PEDOT Derivative with Carboxyl Group and Its Chemo/Bio Sensing Application as Nanocomposite, Immobilized Biological and Enhanced Optical Materials. *Electrochimica Acta* **2014,** *116*, 343-354.

[15] Hu, D.; Zhang, L.; Zhang, K.; Duan, X.; Xu, J.; Dong, L.; Sun, H.; Zhu, X.; Zhen, S., Synthesis and Characterization of PEDOT Derivative with Carboxyl Group and Its Chemo Sensing Application as Enhanced Optical Materials. *Journal of Applied Polymer Science* **2015,** *132*, 41559.

[16] Gulprasertrat, N.; Chapromma, J.; Aree, T.; Sritana-anant, Y., Synthesis of Functionalizable Derivatives of 3,4-ethylenedioxythiophene and Their Solid-State Polymerizations. *Journal of Applied Polymer Science* **2015,** *132*, 42233.

[17] Mawad, D.; Artzy-Schnirman, A.; Tonkin, J.; Ramos, J.; Inal, S.; Mahat, M. M.; Darwish, N.; Zwi-Dantsis, L.; Malliaras, G. G.; Gooding, J. J.; Lauto, A.; Stevens, M. M., Electroconductive Hydrogel Based on Functional Poly(Ethylenedioxy Thiophene). *Chem Mater* **2016,** *28*, 6080-6088.

[18] Bolin, M. H.; Svennersten, K.; Wang, X.; Chronakis, I. S.; Richter-Dahlfors, A.; Jager, E. W. H.; Berggren, M., Nano-Fiber Scaffold Electrodes Based on PEDOT for Cell Stimulation. *Sensors and Actuators B: Chemical* **2009,** *142*, 451-456.

[19] Feng, Z. Q.; Wu, J.; Cho, W.; Leach, M. K.; Franz, E. W.; Naim, Y. I.; Gu, Z. Z.; Corey, J. M.; Martin, D. C., Highly Aligned Poly(3,4-ethylenedioxythiophene) (PEDOT) Nano- and Microscale Fibers and Tubes. *Polymer* **2013,** *54*, 702-708.

[20] Yang, G.; Kampstra, K. L.; Abidian, M. R., High Performance Conducting Polymer Nanofiber Biosensors for Detection of Biomolecules. *Advanced Materials* **2014,** *26*, 4954-4960.

[21] Anastasova, S.; Radu, A.; Matzeu, G.; Zuliani, C.; Mattinen, U.; Bobacka, J.; Diamond, D., Disposable solid-contact ion-selective electrodes for environmental monitoring of lead with ppb limit-of-detection. *Electrochimica Acta* **2012,** *73*, 93-97.

[22] Li, Y.; Hsieh, C. H.; Lai, C. W.; Chang, Y. F.; Chan, H. Y.; Tsai, C. F.; Ho, J. A.; Wu, L. C., Tyramine detection using PEDOT:PSS/AuNPs/1-methyl-4-mercaptopyridine modified screen-printed carbon electrode with molecularly imprinted polymer solid phase extraction. *Biosensors & bioelectronics* **2017,** *87*, 142-149.

[23] Feito, R. F.; Dinsdale, R. M.; Guwy, A. J.; Premier, G. C., Applicability of a PEDOT coated electrode for amperometric quantification of short chain carboxylic acids. *Sensors and Actuators B: Chemical* **2018,** *255*, 712-719.

[24] Wong, A.; Santos, A. M.; Fatibello-Filho, O., Simultaneous determination of paracetamol and levofloxacin using a glassy carbon electrode modified with carbon black, silver nanoparticles and PEDOT:PSS film. *Sensors and Actuators B: Chemical* **2018,** *255*, 2264-2273.

[25] Supaphol, P.; Chuangchote, S., On the electrospinning of poly(vinyl alcohol) nanofiber mats: A revisit. *Journal of Applied Polymer Science* **2008,** *108*, 969-978.

[26] Itoh, H.; Li, Y.; Chan, K. H. K.; Kotaki, M., Morphology and mechanical properties of PVA nanofibers spun by free surface electrospinning. *Polymer Bulletin* **2016,** *73*, 2761-2777.

[27] Sagitha, P.; Sarada, K.; Muraleedharan, K., One-pot synthesis of poly vinyl alcohol (PVA) supported silver nanoparticles and its efficiency in catalytic

reduction of methylene blue. *Transactions of Nonferrous Metals Society of China* **2016,** *26*, 2693-2700.

[28] Liang, K.-L.; Wang, Y.-C.; Lin, W.-L.; Lin, J.-J., Polymer-assisted self-assembly of silver nanoparticles into interconnected morphology and enhanced surface electric conductivity. *RSC Advances* **2014,** *4*, 15098.

[29] Xu, Q.; Li, Y.; Feng, W.; Yuan, X., Fabrication and electrochemical properties of polyvinyl alcohol/poly(3,4-ethylenedioxythiophene) ultrafine fibers via electrospinning of EDOT monomers with subsequent in situ polymerization. *Synthetic Metals* **2010,** *160*, 88-93.

[30] Qin, X. H.; Yang, E. L.; Li, N.; Wang, S. Y., Effect of different salts on electrospinning of polyacrylonitrile (PAN) polymer solution. *Journal of Applied Polymer Science* **2006,** *103*, 3865-3870.

[31] Zong, X.; Kim, K.; Fang, D.; Ran, S.; Hsiao, B. S.; Chu, B., Structure and process relationship of electrospun bioabsorbable nanofiber membranes. *Polymer* **2002,** *43*, 4403-4412.

[32] Moon, K.-S.; Dong, H.; Maric, R.; Pothukuchi, S.; Hunt, A.; Li, Y.; Wong, C. P., Thermal behavior of silver nanoparticles for low-temperature interconnect applications. *Journal of Electronic Materials* **2005,** *34*, 168-175.

[33] Kameda, K., Activities of Liquid Gold-Zinc and Silver-Zinc Binary Alloys by E.M.F. Measurements Using Zirconia Solid Electrolyte Cells. *Transactions of the Japan Institute of Metals* **1987,** *28*, 41-47.

[34] Dirkse, T. P.; Vrieland, E. G., A Study of the Zinc-Noble Metal Couple in Alkaline Solutions. *Journal of The Electrochemical Society* **1959,** *106*, 997-999.

[35] Milchev, A.; Staikov, G., Atomistic Aspects of Electrochemical Alloy Formation: A Review of Nucleation and Growth of Nano-Clusters and Thin Films. *ChemInform* **2005,** *36*.

[36] Živković, D.; Živković, Ž.; Liu, Y. H., Comparative study of thermodynamic predicting methods applied to the Pb–Zn–Ag system. *Journal of Alloys and Compounds* **1998,** *265*, 176-184.

[37] Rico, M. Á. G.; Olivares-Marín, M.; Gil, E. P., Modification of carbon screen-printed electrodes by adsorption of chemically synthesized Bi nanoparticles for the voltammetric stripping detection of Zn(II), Cd(II) and Pb(II). *Talanta* **2009,** *80*, 631-635.

[38] Li, M.; Li, D.-W.; Li, Y.-T.; Xu, D.-K.; Long, Y.-T., Highly selective in situ metal ion determination by hybrid electrochemical "adsorption–desorption" and colorimetric methods. *Analytica Chimica Acta* **2011,** *701*, 157-163.

[39] Ouyang, R.; Zhu, Z.; Tatum, C. E.; Chambers, J. Q.; Xue, Z.-L., Simultaneous stripping detection of Zn(II), Cd(II) and Pb(II) using a bimetallic Hg–Bi/single-walled carbon nanotubes composite electrode. *Journal of Electroanalytical Chemistry* **2011,** *656*, 78-84.

[40] Injang, U.; Noyrod, P.; Siangproh, W.; Dungchai, W.; Motomizu, S.; Chailapakul, O., Determination of trace heavy metals in herbs by sequential injection analysis-anodic stripping voltammetry using screen-printed carbon nanotubes electrodes. *Anal Chim Acta* **2010,** *668*, 54-60.

[41] Xiao, L.; Xu, H.; Zhou, S.; Song, T.; Wang, H.; Li, S.; Gan, W.; Yuan, Q., Simultaneous detection of Cd(II) and Pb(II) by differential pulse anodic stripping voltammetry at a nitrogen-doped microporous carbon/Nafion/bismuth-film electrode. *Electrochimica Acta* **2014,** *143*, 143-151.

[42] Manisankar, P.; Vedhi, C.; Selvanathan, G.; Arumugam, P., Differential pulse stripping voltammetric determination of heavy metals simultaneously using new polymer modified glassy carbon electrodes. *Microchimica Acta* **2008,** *163*, 289-295.

[43] NATIONAL PRIMARY DRINKING WATER REGULATIONS. *Code of Federal Regulations*; Part 141, Title 40.

[44] NATIONAL SECONDARY DRINKING WATER REGULATIONS. *Code of Federal Regulations*; Part 143, Title 40.

APPENDIX

Calculation of percentage of components in electrospun fiber from TGA thermogram

Table A-1 The percentage of remaining ashes of all samples obtained from TGA thermograms

Sample	%Ash
PVA	9.4
PVA/AgNPs	14.8
PEDOT	26.3
PEDOT/PVA	16.8
PEDOT/PVA/AgNPs	19.2

The calculations of percentage of components were performed under the assumption that degradation of PVA and PEDOT leave the same amount of ashes as the pure sample. Percentage of each component was calculated by the following equation:

$$\%Ash = \frac{Ax}{100} + \frac{B(100 - x)}{100}$$

In which %Ash is percentage of remaining ash in that sample, A and B are percentage of remaining ash in pure sample A and B, respectively, and x is the percentage of component A in the sample.

VITA

Mr. Thanarath Pisuchpen was born on October 15th, 1986 in Bangkok, Thailand. He received the Degree of Bachelor of Science (Chemistry), Faculty of Science, Chulalongkorn University, Pathumwan, Bangkok, Thailland in 2009 and Master of Science (Chemistry), Faculty of Science, Chulalongkorn University, Pathumwan, Bangkok, Thailland in 2012. In the same year, He was admitted to a Doctoral Degree in Program of Chemistry, Faculty of Science, Chulalongkorn University and completed the program in 2018. His address is 9, Phahon Yothin 17, Thanon Phahon Yothin, Chatuchak, Bangkok 10900.

Publication:

Pisuchpen, T.; Chaim-ngoen, N.; Intasanta, N.; Supaphol, P.; Hoven, V. P. “Tuning Hydrophobicity and Water Adhesion by Electrospinning and Silanization” Langmuir, 2011, 27(7), 3654-3661.

Pisuchpen, T.; Intasanta, V.; Hoven, V. P. “Highly Porous Organic-Inorganic Hybrid Fiber from Copolymers of Styrene and Polyhedral Oligomeric Silsesquioxane-derived Methacrylate: Syntheses, Fiber Formation and Potential Modification” Eur. Polym. J., 2014, 60, 38-48

Pisuchpen, T.; Kaew-on, N.; Kitikulvarakorn, K.; Kusonsong, S.; Sritana-anant, Y.; Supaphol, P.; Hoven, V. P. “Electrospinning and Solid State Polymerization: A New and Versatile Route to Conducting PEDOT-containing Composite Films”, Eur. Polym. J. 2017, 96, 452-462.